Electronic Supplementary Material (ESI) for Journal of Materials Chemistry A.

Electronic Supplementary Materials

Energy harvesting and electricity production through dissolved carbon dioxide by connecting two form-stable phase change materials

Chengbin Yu[a], John Konlan[a], Guoqiang Li[a,b,*]

[a] *Department of Mechanical and Industrial Engineering, Louisiana State University, Baton Rouge, LA 70803, United States of America*
[b] *Department of Mechanical Engineering, Southern University and A &M College, Baton Rouge, LA 70813, United States of America*

***Corresponding author:**

Prof. Guoqiang Li

Department of Mechanical and Industrial Engineering

Louisiana State University

Tel.: +1-225-578-5302;

E-mail address: lguoqi1@lsu.edu

The supplementary figures include the follows:

Fig. S1. (a) Basic equation of carbon dioxide (CO_2) dissolving into the water and (b) design of electrical energy harvesting.

Fig. S2. Procedure of synthesizing cross-linked shape memory vitrimer (SMV) by thermal curing.

Fig. S3. Procedure of synthesizing the final SMV through 3D printing by ultraviolet curing.

Fig. S4. (a) Fabrication of SMV supported PCM composite. (b) Optical images of different size of SMV containers.

Fig. S5. FTIR results of (a) diphenyl carbonate, (b) di(trimethylolpropane), (c) tris(2-aminoethylamine), (d) pre-vitrimer, (e) pre-mixture before 3D printing, and (f) final SMV at different temperature.

Fig. S6. XPS results of diphenyl carbonate at (a) C1s peaks and (b) O1s peaks. The di(trimethylolpropane) at (c) C1s peaks and (d) O1s peaks.

Fig. S7. XPS results of pre-synthesized polymer without mixing with tris((2-(acryloyloxy)ethyl) isocyanurate (TAI) (a) C1s peaks and (b) O1s peaks, and (c) N1s peaks. (d) Atomic spectrum of three elements.

Fig. S8. XPS results of final SMV (a) C1s peaks and (b) O1s peaks, and (c) N1s peaks. (d) Atomic spectrum of three elements.

Fig. S9. Raman peaks of (a) diphenyl carbonate, (b) di(trimethylolpropane), (c) pre-vitrimer, (d) final SMV.

Fig. S10. (a) Stress-strain curves of pre-vitrimer and final SMV. SEM images of (b) final SMV, (c) pure 1-TD, and (d) pure PEG.

Fig. S11. Form stable test optical images of (a) pure 1-TD and 1-TD composites, and (b) pure PEG and PEG composites.

Fig. S12. Volume expansion ratios of (a) SMV supported 1-TD composite and (b) SMV supported PEG composite. (c) thermal conductivity results of pure PCM and PCM composites. (d) XRD peaks of SMV, pure PCM, and PCM composites.

Fig. S13. DSC cycling results of (a) SMV, (b) pure -1TD, and (c) pure PEG. (d) XRD peaks after 100 cycles.

Fig. S14. (a) The final temperature with different RH at 15 mW/cm^2 solar light intensity. Electrical resistivity peaks of (b) RH 70% with initial 400 ppm CO_2 concentration, (c) RH 80% with initial 400 ppm CO_2 concentration, and (d) RH 90% with initial 400 ppm CO_2 concentration.

Fig. S15. Electrical resistivity peaks of (a) RH 70% with 700 ppm CO_2 concentration, (b) RH 80% with initial 700 ppm CO_2 concentration, (c) RH 90% with initial 700 ppm CO_2 concentration, (d) RH 70% with initial 1200 ppm CO_2 concentration, (e) RH 80% with initial 1200 ppm CO_2 concentration, and (f) RH 90% with initial 1200 ppm CO_2 concentration.

Fig. S16. The electrical resistivity at RH 70%, the different thickness of SMV supported 1-TD composite under (a) 400 ppm CO_2 concentration, (b) 700 ppm CO_2 concentration, (c) 1200 ppm CO_2 concentration. For the different thickness of SMV supported PEG composites under (d) 400 ppm CO_2 concentration, (e) 700 ppm CO_2 concentration, and (f) 1200 ppm CO_2 concentration.

Fig. S17. The electrical resistivity at RH 80%, the different thickness of SMV supported 1-TD composite under (a) 400 ppm CO_2 concentration, (b) 700 ppm CO_2 concentration, (c) 1200 ppm CO_2 concentration. For the different thickness of SMV supported PEG composites under (d) 400 ppm CO_2 concentration, (e) 700 ppm CO_2 concentration, and (f) 1200 ppm CO_2 concentration.

Fig. S18. The electrical resistivity at RH 90%, the different thickness of SMV supported 1-TD composite under (a) 400 ppm CO_2 concentration, (b) 700 ppm CO_2 concentration, (c) 1200 ppm CO_2 concentration. For the different thickness of SMV supported PEG composites under (d) 400 ppm CO_2 concentration, (e) 700 ppm CO_2 concentration, and (f) 1200 ppm CO_2 concentration.

Fig. S19. The temperature peaks of different thickness of SMV supported 1-TD composites, the light-on process at (a) RH 40% with 400 ppm CO_2 concentration, (b) RH 40% with 700 ppm CO_2 concentration, (c) RH 40% with 1200 ppm CO_2 concentration. For light-off process, (d) RH 40% with 400 ppm CO_2 concentration, (e) RH 40% with 700 ppm CO_2 concentration, (f) RH 40% with 1200 ppm CO_2 concentration.

Fig. S20. The temperature peaks of different thickness of SMV supported PEG composites, the light-on process at (a) RH 40% with 400 ppm CO_2 concentration, (b) RH 40% with 700 ppm CO_2 concentration, (c) RH 40% with 1200 ppm CO_2 concentration. For light-off process, (d) RH 40% with 400 ppm CO_2 concentration, (e) RH 40% with 700 ppm CO_2 concentration, (f) RH 40% with 1200 ppm CO_2 concentration.

Fig. S21. The temperature peaks of 3.5 mm height SMV supported 1-TD composite, the light-on process at (a) RH 40% with different CO_2 concentration, (b) RH 70% with different CO_2 concentration, (c) RH 80% with different CO_2 concentration, and (d) RH 90% with different CO_2 concentration. For light-off process, (e) RH 40% with different CO_2 concentration, (f) RH 70% with different CO_2 concentration, (g) RH 80% with different CO_2 concentration, and (h) RH 90% with different CO_2 concentration.

Fig. S22. The temperature peaks of 3.5 mm height SMV supported PEG composite, the light-on process at (a) RH 40% with different CO_2 concentration, (b) RH 70% with different CO_2 concentration, (c) RH 80% with different CO_2 concentration, and (d) RH 90% with different CO_2 concentration. For light-off process, (e) RH 40% with different CO_2 concentration, (f) RH 70% with different CO_2 concentration, (g) RH 80% with different CO_2 concentration, and (h) RH 90% with different CO_2 concentration.

Fig. S23. The assembly made of RH 40% SMV supported 1-TD and RH 40% SMV supported PEG, the light-on process with (a) voltage at different CO_2 concentration (b) current at different CO_2 concentration. For light-off process, (c) voltage at different CO_2 concentration (d) current at different CO_2 concentration.

Fig. S24. The assembly made of RH 40% SMV supported 1-TD and RH 70% SMV supported PEG, the light-on process with (a) voltage at different CO_2 concentration (b) current at different CO_2 concentration. For light-off process, (c) voltage at different CO_2 concentration (d) current at different CO_2 concentration.

Fig. S25. The assembly made of RH 70% SMV supported 1-TD and RH 40% SMV supported PEG, the light-on process with (a) voltage at different CO_2 concentration (b) current at different CO_2 concentration. For light-off process, (c) voltage at different CO_2 concentration (d) current at different CO_2 concentration.

Fig. S26. The assembly made of RH 70% SMV supported 1-TD and RH 80% SMV supported PEG, the light-on process with (a) voltage at different CO_2 concentration (b) current

at different CO_2 concentration. For light-off process, (c) voltage at different CO_2 concentration (d) current at different CO_2 concentration.

Fig. S27. Long-term durability of the assembly made of RH 70% SMV supported 1-TD and RH 80% SMV supported PEG under the 700 ppm CO_2 concentration (a) Output voltage and (b) output current up to 5 cycles upon light-on process. (c) Output voltage and (d) output current up to 5 cycles upon light-off process.

Fig. S28. Long-term durability of the assembly made of RH 70% SMV supported 1-TD and RH 80% SMV supported PEG under the 1200 ppm CO_2 concentration (a) Output voltage and (b) output current up to 5 cycles upon light-on process. (c) Output voltage and (d) output current up to 5 cycles upon light-off process.

Fig. S29. The assembly made of RH 80% SMV supported 1-TD and RH 70% SMV supported PEG, the light-on process with (a) voltage at different CO_2 concentration (b) current at different CO_2 concentration. For light-off process, (c) voltage at different CO_2 concentration (d) current at different CO_2 concentration.

Fig. S30. Long-term durability of the assembly made of RH 80% SMV supported 1-TD and RH 70% SMV supported PEG under the 700 ppm CO_2 concentration (a) Output voltage and (b) output current up to 5 cycles upon light-on process. (c) Output voltage and (d) output current up to 5 cycles upon light-off process.

Fig. S31. Long-term durability of the assembly made of RH 80% SMV supported 1-TD and RH 70% SMV supported PEG under the 1200 ppm CO_2 concentration (a) Output voltage and (b) output current up to 5 cycles upon light-on process. (c) Output voltage and (d) output current up to 5 cycles upon light-off process.

Fig. S32. The assembly made of RH 80% SMV supported 1-TD and RH 90% SMV supported PEG, the light-on process with (a) voltage at different CO_2 concentration (b) current at different CO_2 concentration. For light-off process, (c) voltage at different CO_2 concentration (d) current at different CO_2 concentration.

Fig. S33. Long-term durability of the assembly made of RH 80% SMV supported 1-TD and RH 90% SMV supported PEG under the 700 ppm CO_2 concentration (a) Output voltage and (b) output current up to 5 cycles upon light-on process. (c) Output voltage and (d) output current up to 5 cycles upon light-off process.

Fig. S34. Long-term durability of the assembly made of RH 80% SMV supported 1-TD and RH 90% SMV supported PEG under the 1200 ppm CO_2 concentration (a) Output voltage and (b) output current up to 5 cycles upon light-on process. (c) Output voltage and (d) output current up to 5 cycles upon light-off process.

Fig. S35. The assembly made of RH 90% SMV supported 1-TD and RH 80% SMV supported PEG, the light-on process with (a) voltage at different CO_2 concentration (b) current at different CO_2 concentration. For light-off process, (c) voltage at different CO_2 concentration (d) current at different CO_2 concentration.

Fig. S36. Long-term durability of the assembly made of RH 90% SMV supported 1-TD and RH 80% SMV supported PEG under the 700 ppm CO_2 concentration (a) Output voltage and (b) output current up to 5 cycles upon light-on process. (c) Output voltage and (d) output current up to 5 cycles upon light-off process.

Fig. S37. Long-term durability of the assembly made of RH 90% SMV supported 1-TD and RH 80% SMV supported PEG under the 1200 ppm CO_2 concentration (a) Output voltage and

(b) output current up to 5 cycles upon light-on process. (c) Output voltage and (d) output current up to 5 cycles upon light-off process.

Fig. S38. Long-term durability of the assembly made of RH 70% SMV supported 1-TD and RH 90% SMV supported PEG under the 700 ppm CO_2 concentration (a) Output voltage and (b) output current up to 5 cycles upon light-on process. (c) Output voltage and (d) output current up to 5 cycles upon light-off process.

Fig. S39. Long-term durability of the assembly made of RH 70% SMV supported 1-TD and RH 90% SMV supported PEG under the 1200 ppm CO_2 concentration (a) Output voltage and (b) output current up to 5 cycles upon light-on process. (c) Output voltage and (d) output current up to 5 cycles upon light-off process.

Fig. S40. The assembly made of RH 90% SMV supported 1-TD and RH 70% SMV supported PEG, the light-on process with (a) voltage at different CO_2 concentration (b) current at different CO_2 concentration. For light-off process, (c) voltage at different CO_2 concentration (d) current at different CO_2 concentration.

Fig. S41. Long-term durability of the assembly made of RH 90% SMV supported 1-TD and RH 70% SMV supported PEG under the 700 ppm CO_2 concentration (a) Output voltage and (b) output current up to 5 cycles upon light-on process. (c) Output voltage and (d) output current up to 5 cycles upon light-off process.

Fig. S42. Long-term durability of the assembly made of RH 90% SMV supported 1-TD and RH 70% SMV supported PEG under the 1200 ppm CO_2 concentration (a) Output voltage and (b) output current up to 5 cycles upon light-on process. (c) Output voltage and (d) output current up to 5 cycles upon light-off process.

Fig. S43. The assembly made of RH 70% SMV supported 1-TD and RH 90% SMV supported PEG, the temperature profiles of 700 ppm and 1200 ppm two different CO_2 concentrations during (a) light-on process and (b) light-off process.

Fig. S44. The comparison of simulated result, temperature peaks during the light-on process with (a) 700 ppm CO_2 concentration and (b) 1200 ppm CO_2 concentration. For light-off process, (c) 700 ppm CO_2 concentration and (d) 1200 ppm CO_2 concentration. (e) The energy harvesting efficiency results at 700 ppm and 1200 ppm CO_2 concentration during light-on/-off process.

Numerical analysis

The temperature profiles of PCM composites are calculated by the finite element modeling (FEM) by using commercial software package COMSOL Multiphysics. The solar-to-electrical energy harvesting device was composed of SMV supported 1-TD and PEG composites. It is confirmed that the temperature difference triggers the Seebeck effect which can generate electron movements in the closed circuit. The finite element mesh was generated according to the experimental specimen and the model consisted of SMV supported 1-TD and PEG composites. The different electrical conductivity between 1-TD and PEG composites is crucial to generating the Seebeck effect and utilized as a parameter to run the simulation. Furthermore, latent heat (ΔH), thermal conductivity, and temperature peaks (T_m, T_c) of the two PCM composites were input to calculate the temperature gradients during the light-on/-off process. The solar-to-electrical energy harvesting was conducted in a simulation space with 15 mW/cm^2 sunlight and the temperature was increased from the initial 25 °C to the final 80 °C during the light-on process. After removing the light source, the cooling process was started under the natural cooling condition, and the temperature was decreased rapidly during the light-off process. The total mesh elements were 32348 and the model of the heat transfer governing equation is defined as:

$$\rho C_p \frac{\partial T}{\partial t} + \rho C_p u \cdot \nabla T + \nabla \cdot q = Q \qquad \text{Eqn (1)}$$

$$C_p = \frac{1}{\rho}\left(\theta \rho_{phase1} C_{p.phase1} + (1-\theta)\rho_{phase2} C_{p.phase2}\right) + L\frac{\partial \alpha_m}{\partial T} \qquad \text{Eqn (2)}$$

$$k = \theta k_{phase1} + (1-\theta) k_{phase2} \qquad \text{Eqn (3)}$$

$$\alpha_m = \frac{1}{2}\frac{(1-\theta)\rho_{phase2} - \theta\rho_{phase1}}{\theta\rho_{phase1} + (1-\theta)\rho_{phase2}} \qquad \text{Eqn (4)}$$

where, ρ is mass density and C_p means heat capacity. The heat transfer rate q is correlated to the thermal conductivity k and the temperature variation is a function of the heat transfer rate as $q = -k\nabla T$. The phase transition of PCM composite is normally defined as $\rho = \theta\rho_{phase1} + (1-\theta)\rho_{phase2}$ where the fitting-factor θ can be modified by following typical parameters (C_p, k, and α_m) in Eqn (4). Mass coefficient is α_m and the normal vector n and heat transfer rate $-n \cdot q = q_0$ show the external heat convection boundary condition after absorbing the sunlight. q_0 refers to the convection heat flux and Eqn (5) shows the relationship between heat transfer coefficient (h_{air}) as below:

$$q_0 = h_{air} \cdot (T_{ext} - T) \qquad \text{Eqn (5)}$$

The Seebeck coefficient S is utilized to calculate the output electrical voltage V and the equation is shown as $V = S \cdot \Delta T$. The output electrical current can be calculated from the Seebeck coefficient S, and temperature difference (ΔT) as $I = \frac{S\Delta T}{R}$; where R refers to the electrical resistance of the SMV supported PCM composites.

The solar-to-electrical energy harvesting efficiency η is correlated to the converted energy W and the PCM stored energy Q during the light-on/-off process as defined:

$$\eta = \frac{W}{Q} \qquad \text{Eqn (6)}$$

Supplementary Figures and Tables

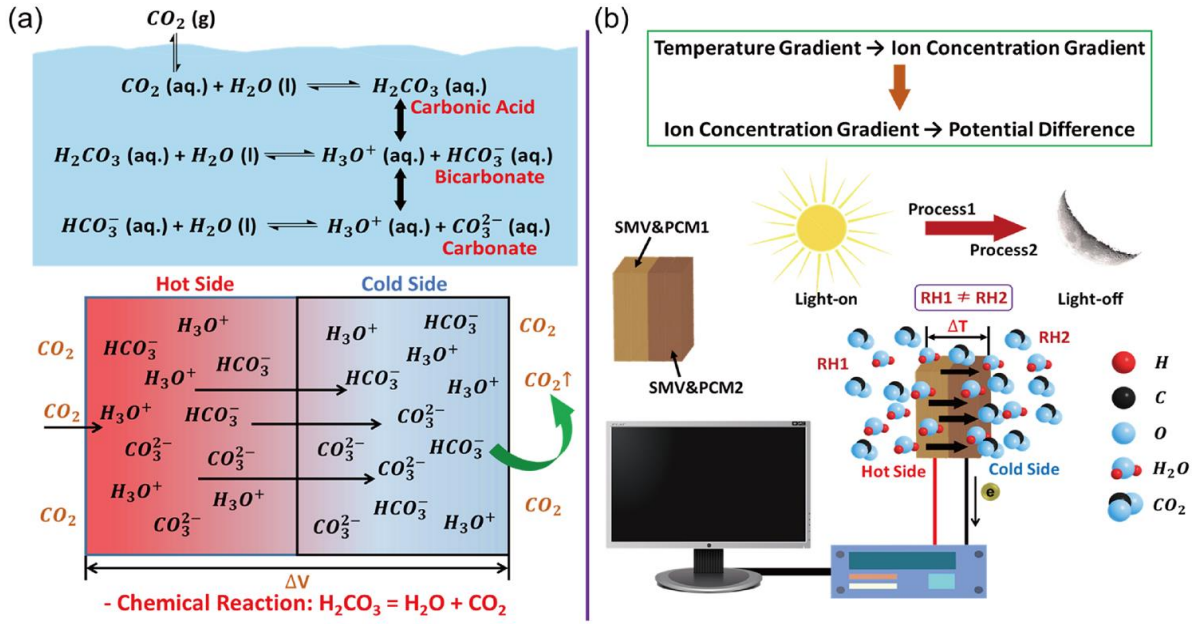

Fig. S1. (a) Basic equation of carbon dioxide (CO_2) dissolving into the water and (b) design of electrical energy harvesting.

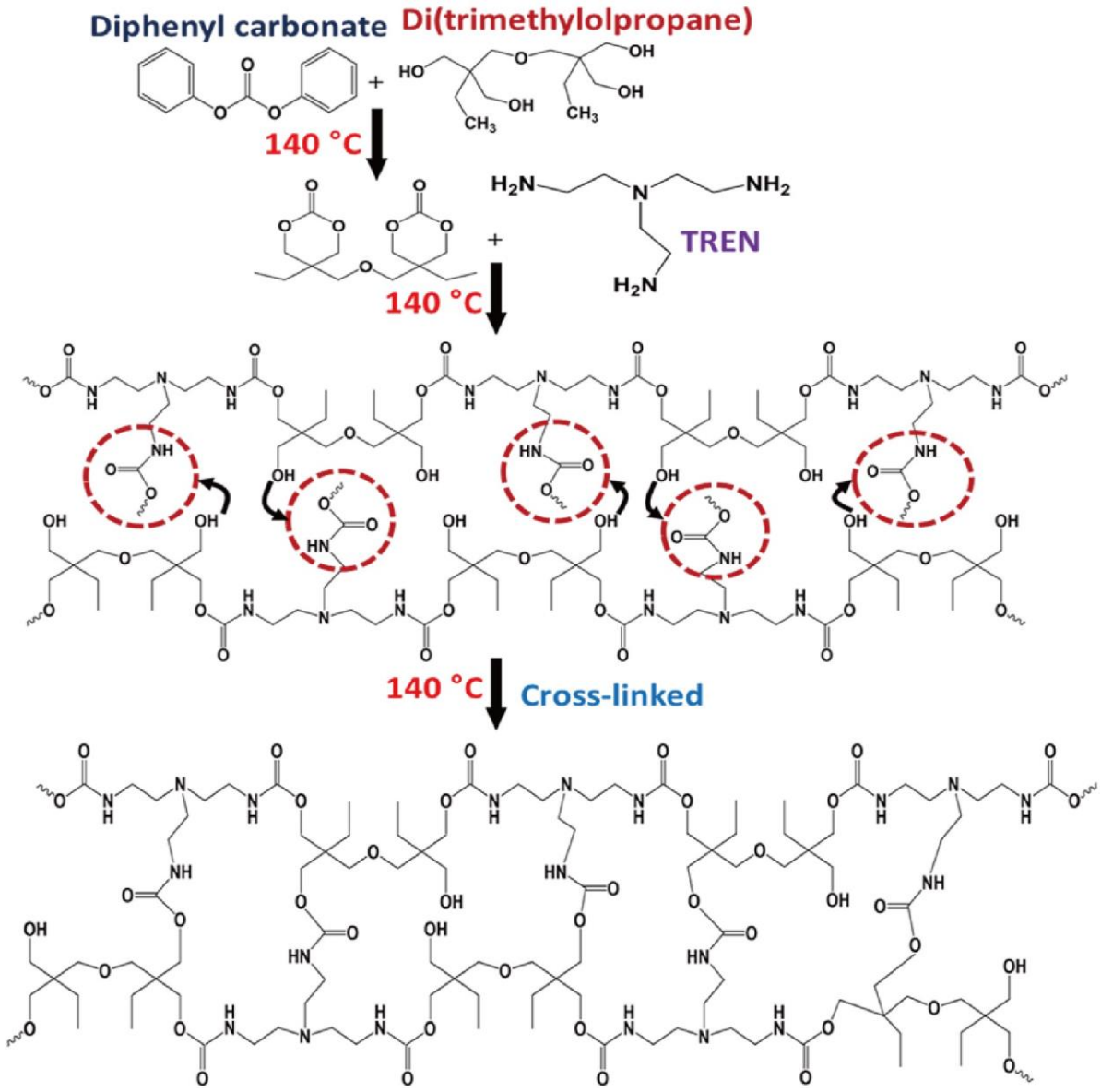

Fig. S2. Procedure of synthesizing cross-linked shape memory vitrimer (SMV) by thermal curing.

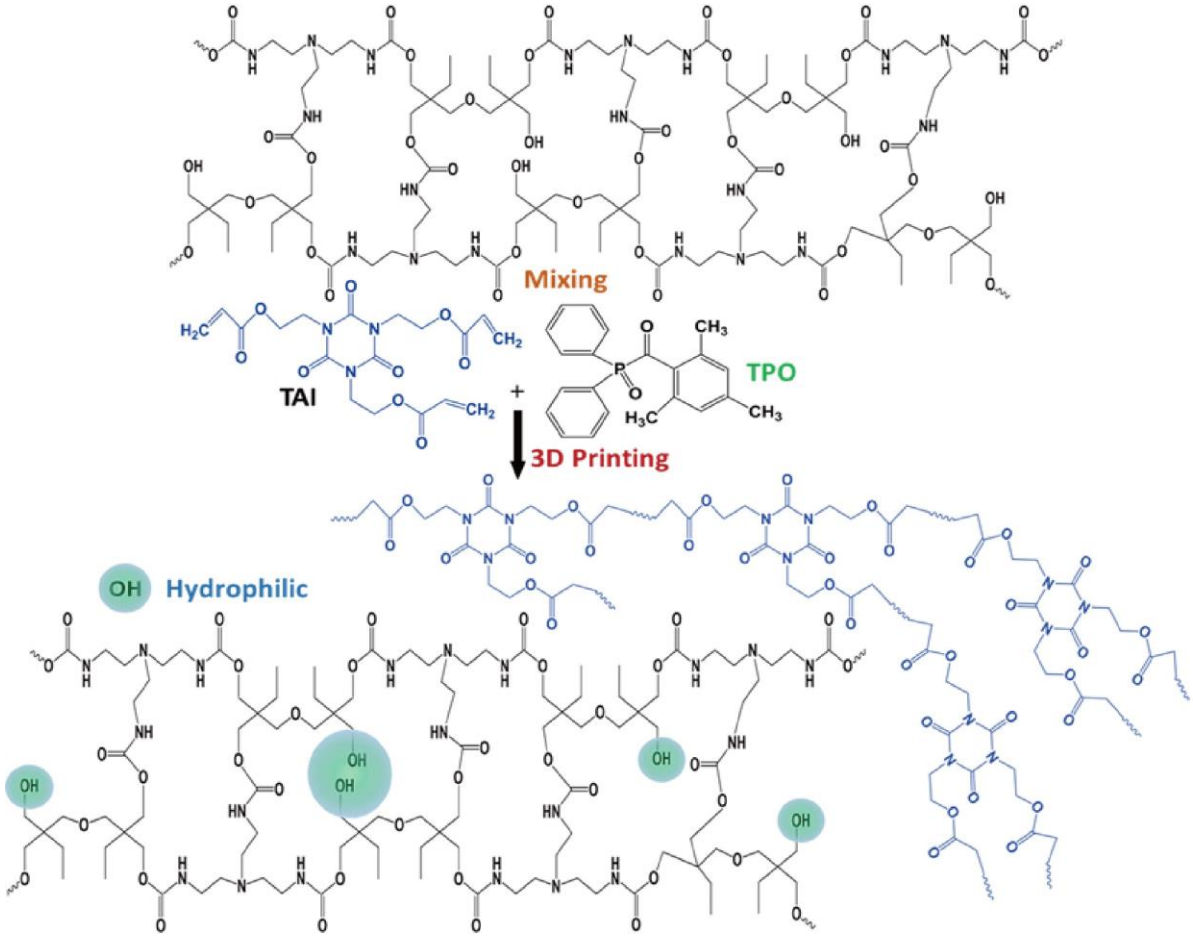

Fig. S3. Procedure of synthesizing the final SMV through 3D printing by ultraviolet curing.

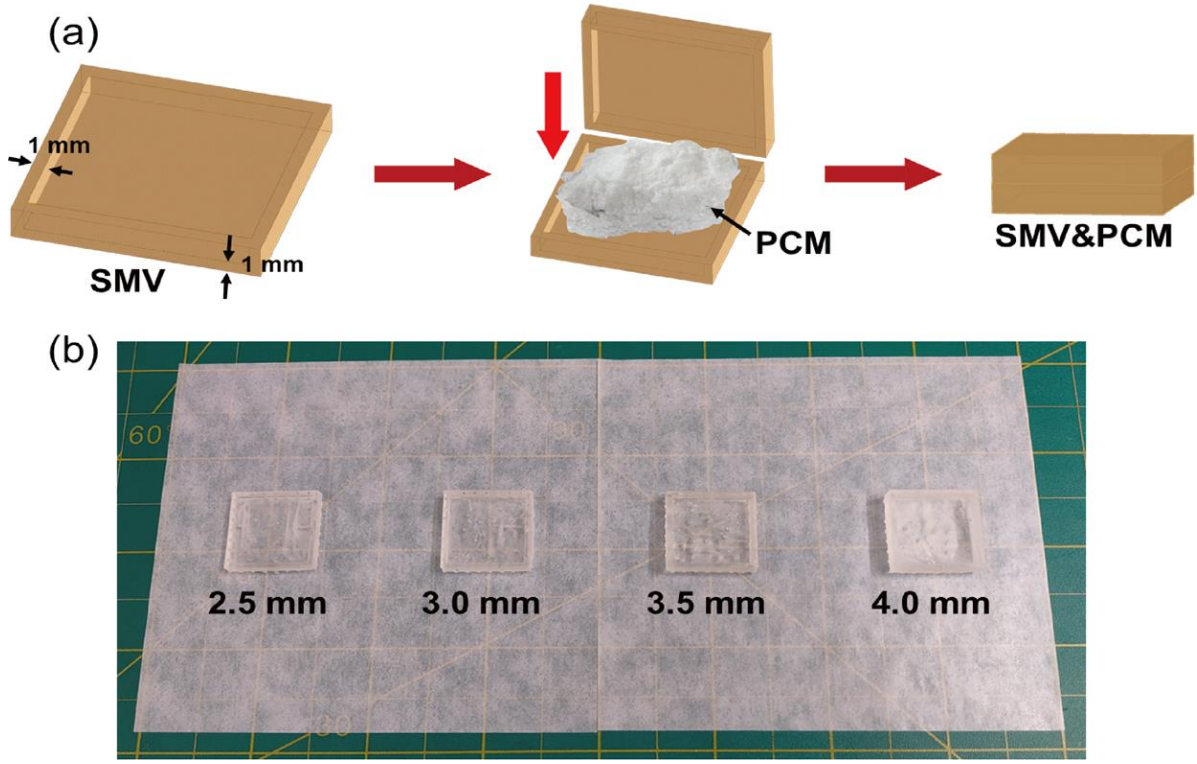

Fig. S4. (a) Fabrication of SMV supported PCM composite. (b) Optical images of different size of SMV containers.

Table S1. Weight of SMV containers, pure PCMs and final PCM composites.

Weight	SMV container	Pure PCM		SMV container × 2 + PCM + SMV coating	
		1-TD	PEG	1-TD	PEG
2.5 mm	1.250 g	0.801 g	1.159 g	3.541 g	3.880 g
3.0 mm	1.336 g	1.068 g	1.559 g	4.039 g	4.532 g
3.5 mm	1.465 g	1.338 g	1.940 g	4.606 g	5.191 g
4.0 mm	1.547 g	1.562 g	2.329 g	5.002 g	5.774 g

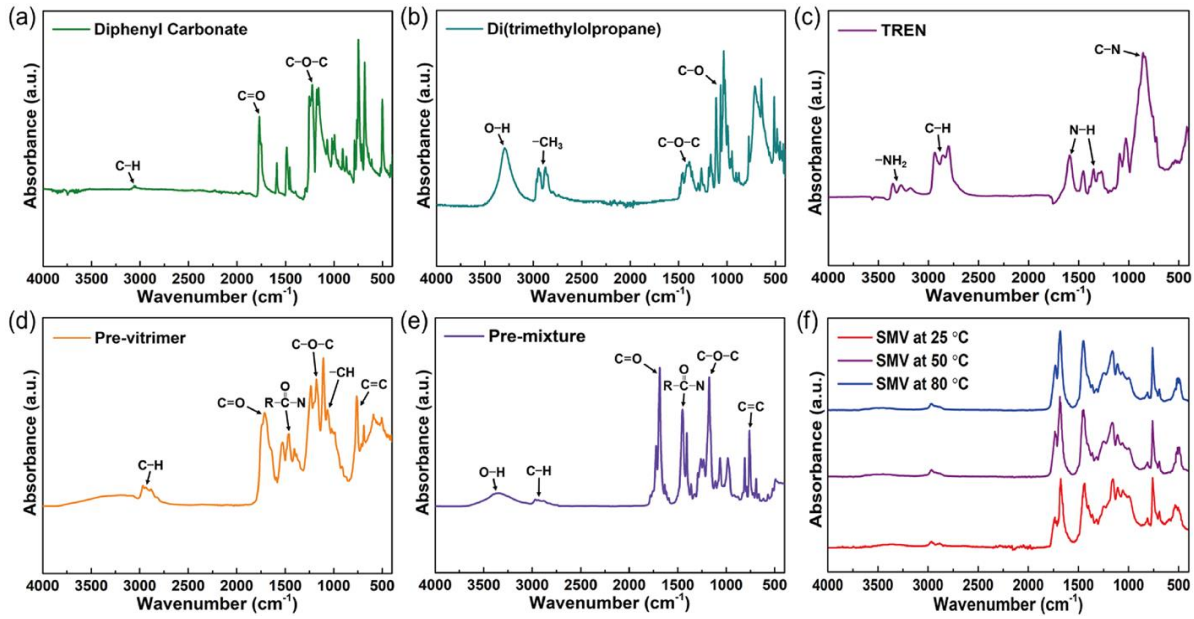

Fig. S5. FTIR results of (a) diphenyl carbonate, (b) di(trimethylolpropane), (c) tris(2-aminoethylamine), (d) pre-vitrimer, (e) pre-mixture before 3D printing, and (f) final SMV at different temperature.

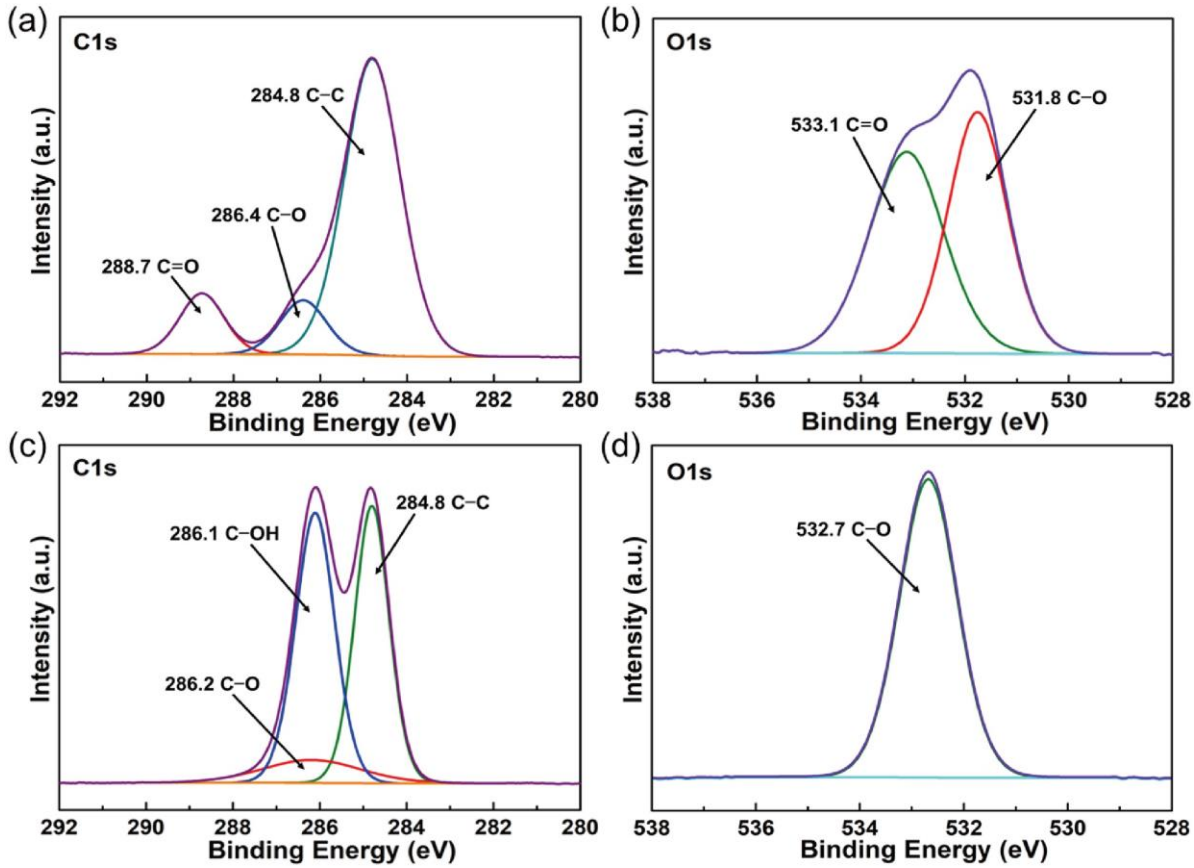

Fig. S6. XPS results of diphenyl carbonate at (a) C1s peaks and (b) O1s peaks. The di(trimethylolpropane) at (c) C1s peaks and (d) O1s peaks.

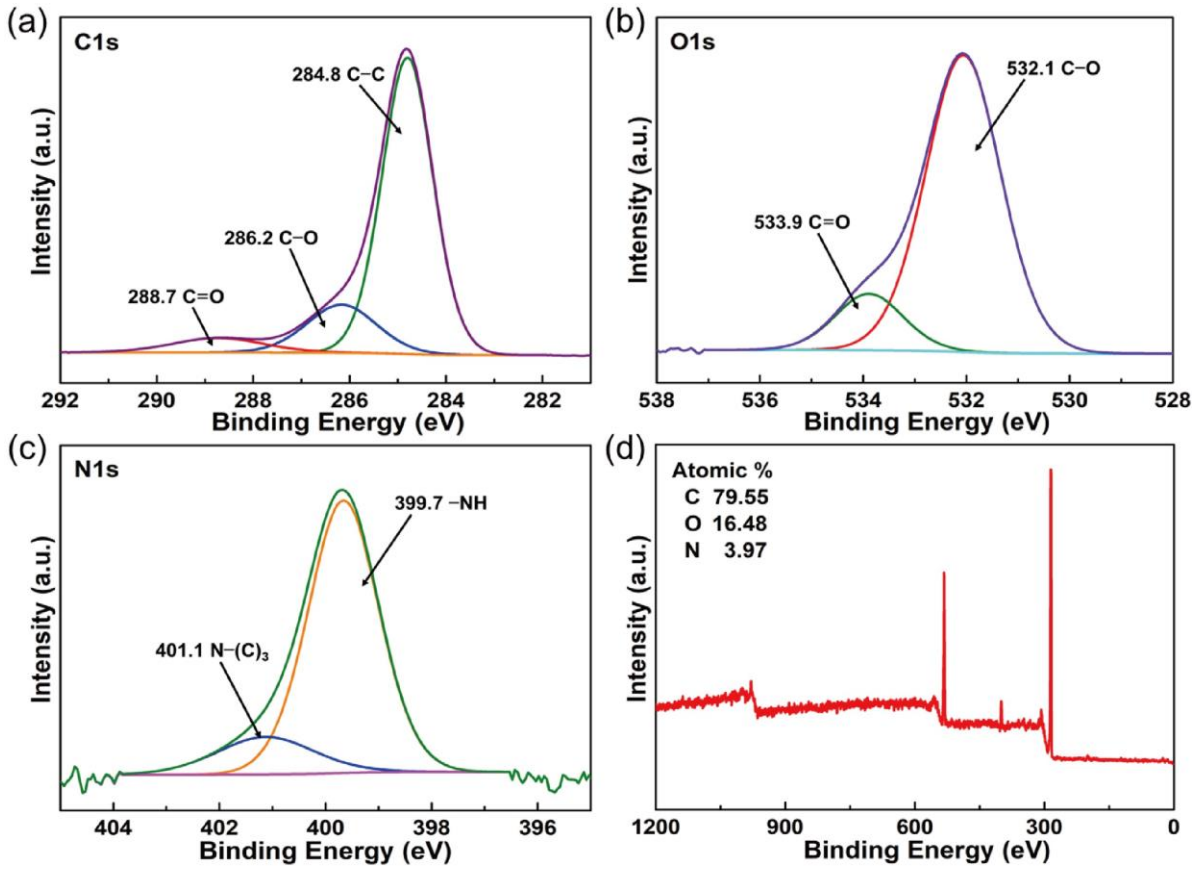

Fig. S7. XPS results of pre-synthesized polymer without mixing with tris((2-(acryloyloxy)ethyl) isocyanurate (TAI) (a) C1s peaks and (b) O1s peaks, and (c) N1s peaks. (d) Atomic spectrum of three elements.

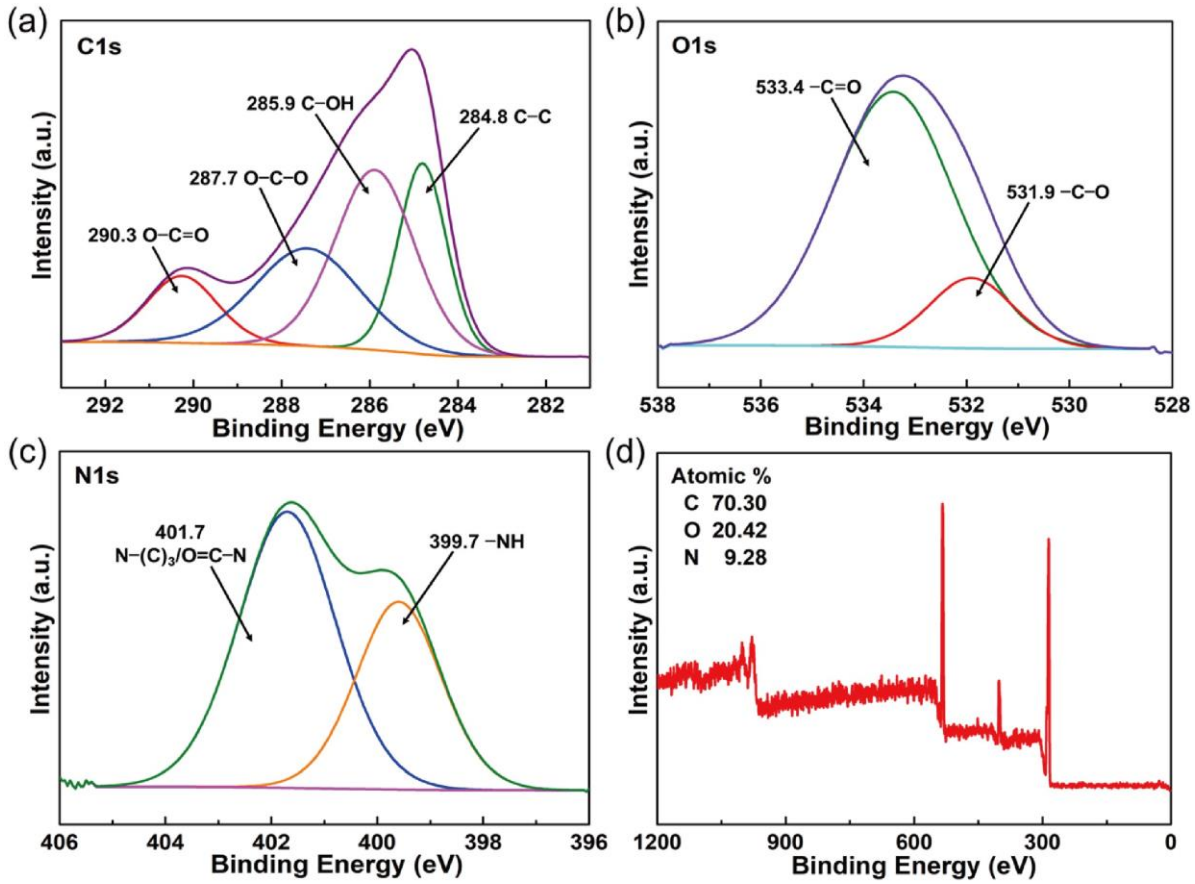

Fig. S8. XPS results of final SMV (a) C1s peaks and (b) O1s peaks, and (c) N1s peaks. (d) Atomic spectrum of three elements.

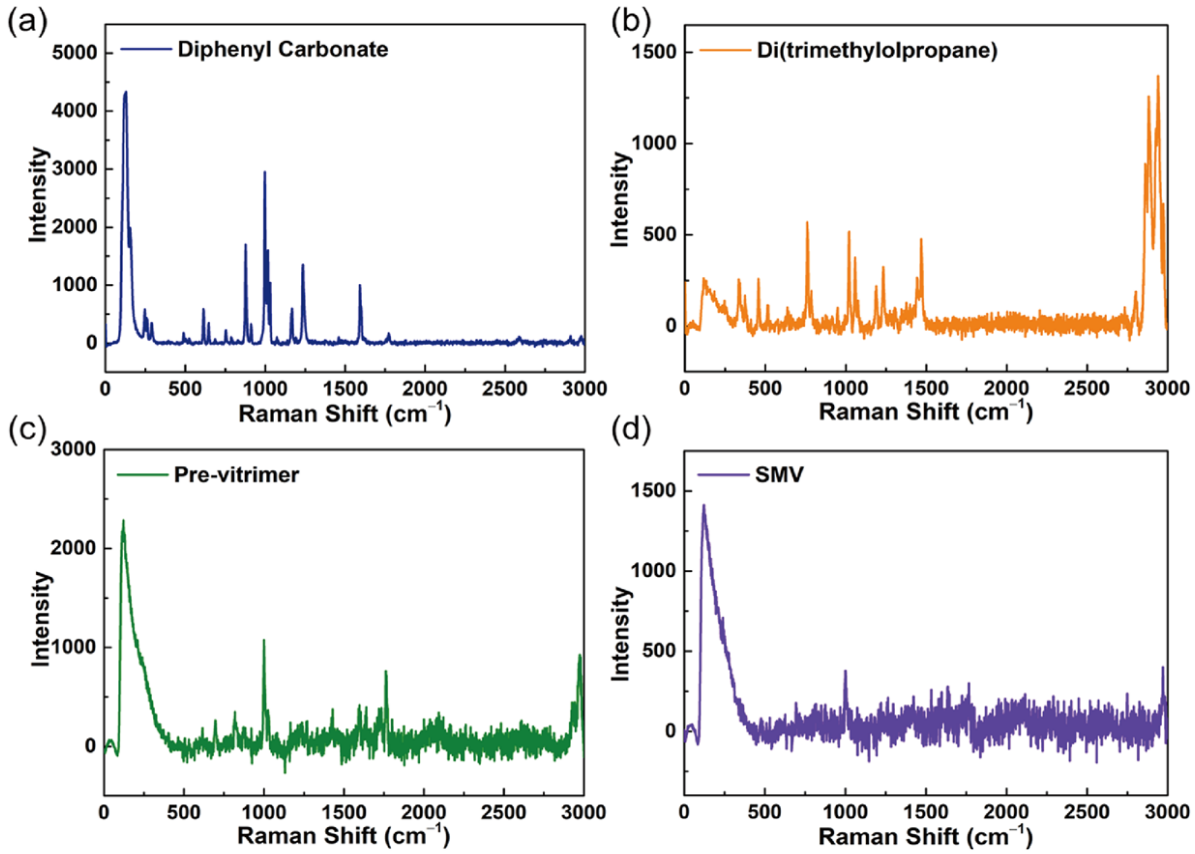

Fig. S9. Raman peaks of (a) diphenyl carbonate, (b) di(trimethylolpropane), (c) pre-vitrimer, (d) final SMV.

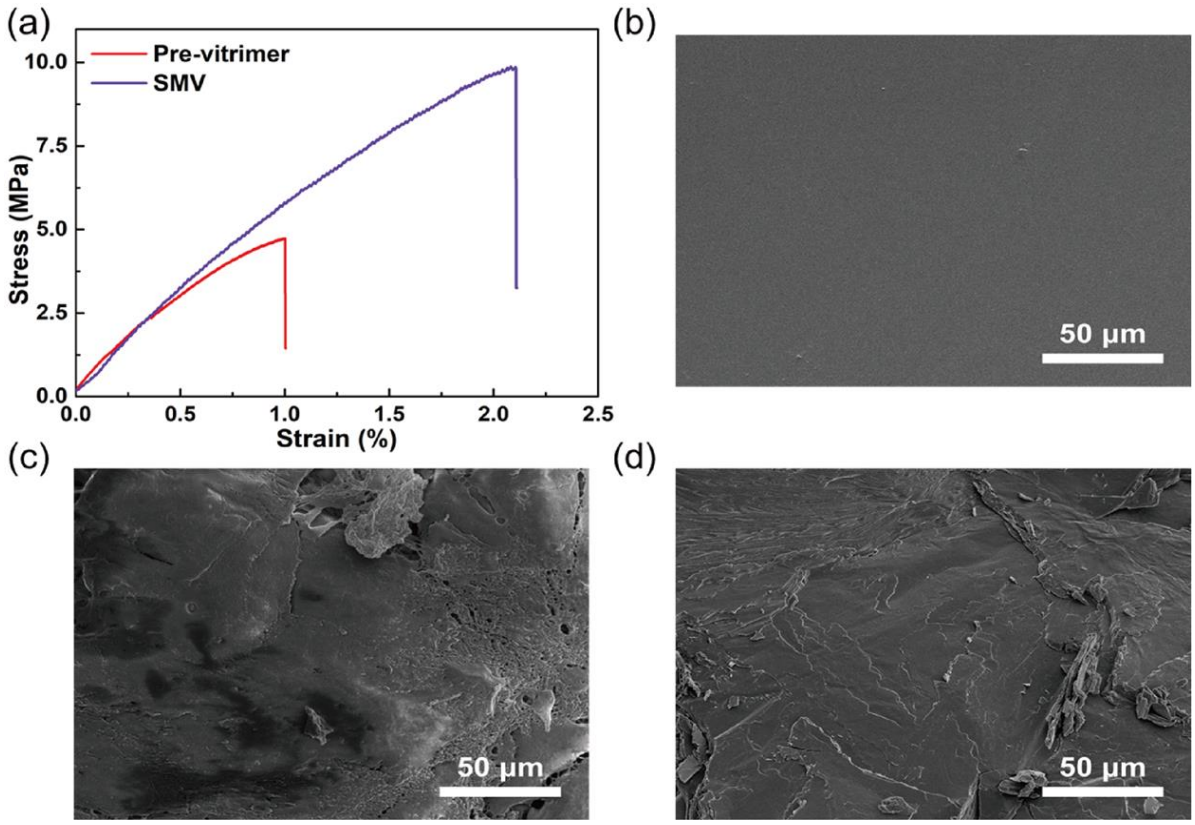

Fig. S10. (a) Stress-strain curves of pre-vitrimer and final SMV. SEM images of (b) final SMV, (c) pure 1-TD, and (d) pure PEG.

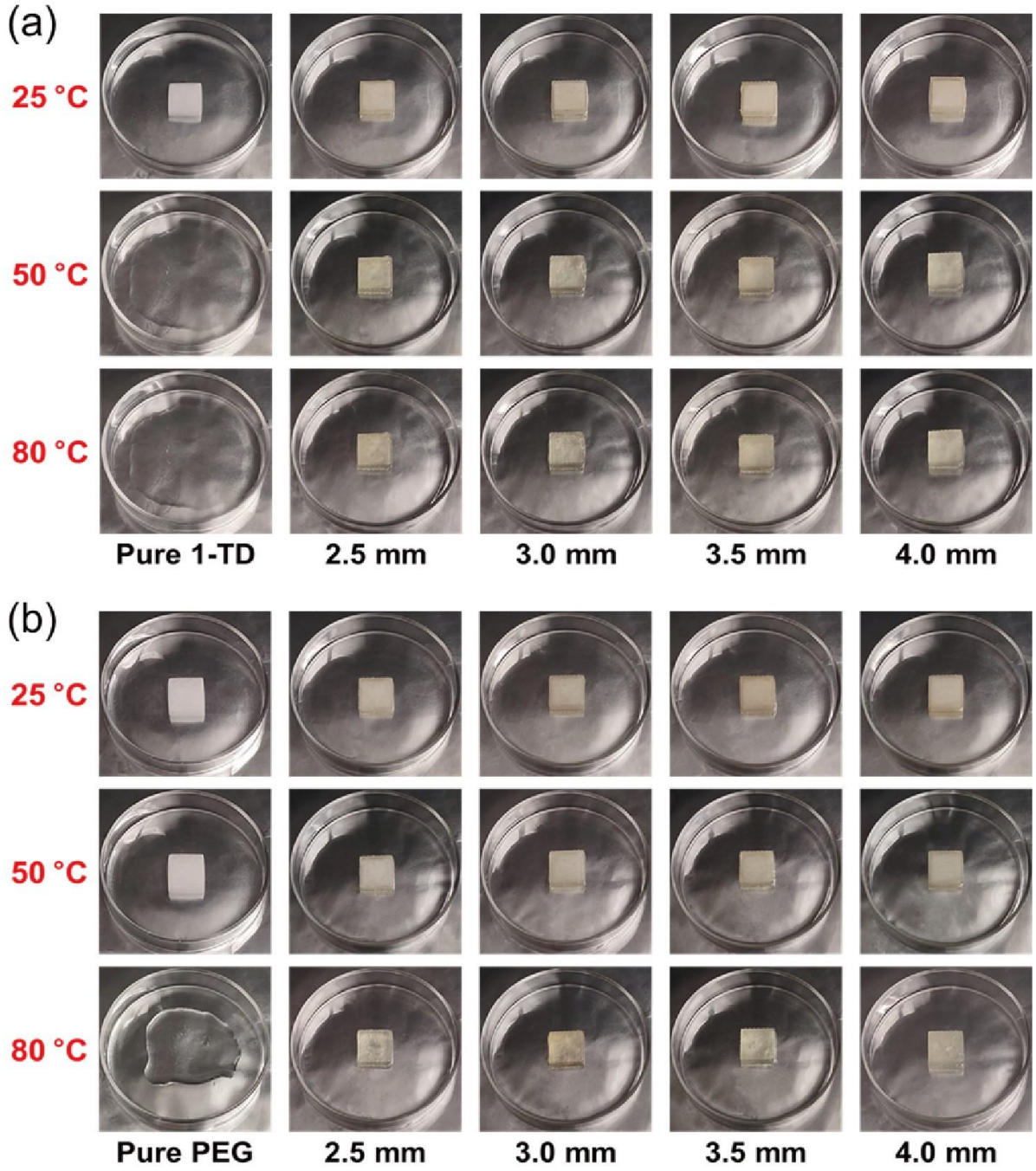

Fig. S11. Form stable test optical images of (a) pure 1-TD and 1-TD composites, and (b) pure PEG and PEG composites.

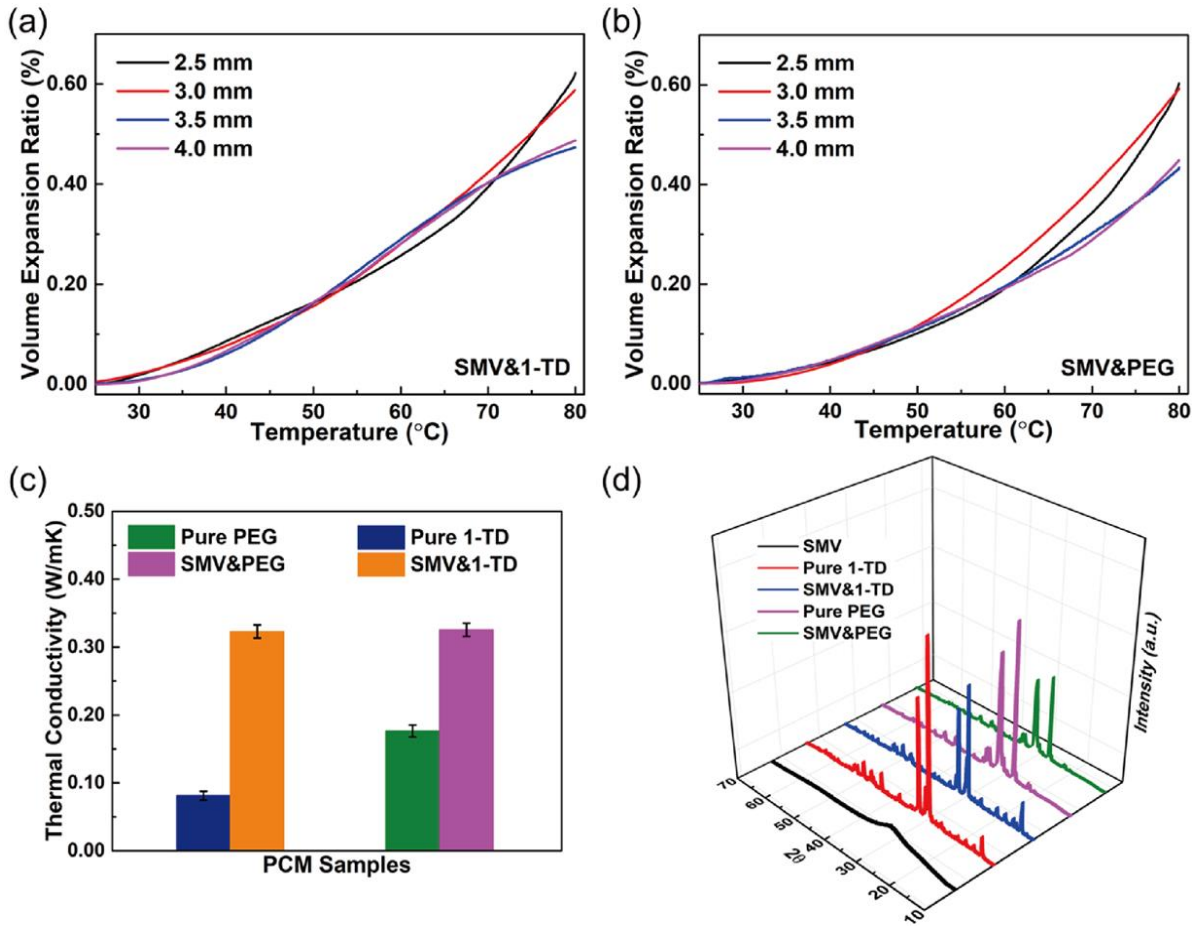

Fig. S12. Volume expansion ratios of (a) SMV supported 1-TD composite and (b) SMV supported PEG composite. (c) thermal conductivity results of pure PCM and PCM composites. (d) XRD peaks of SMV, pure PCM, and PCM composites.

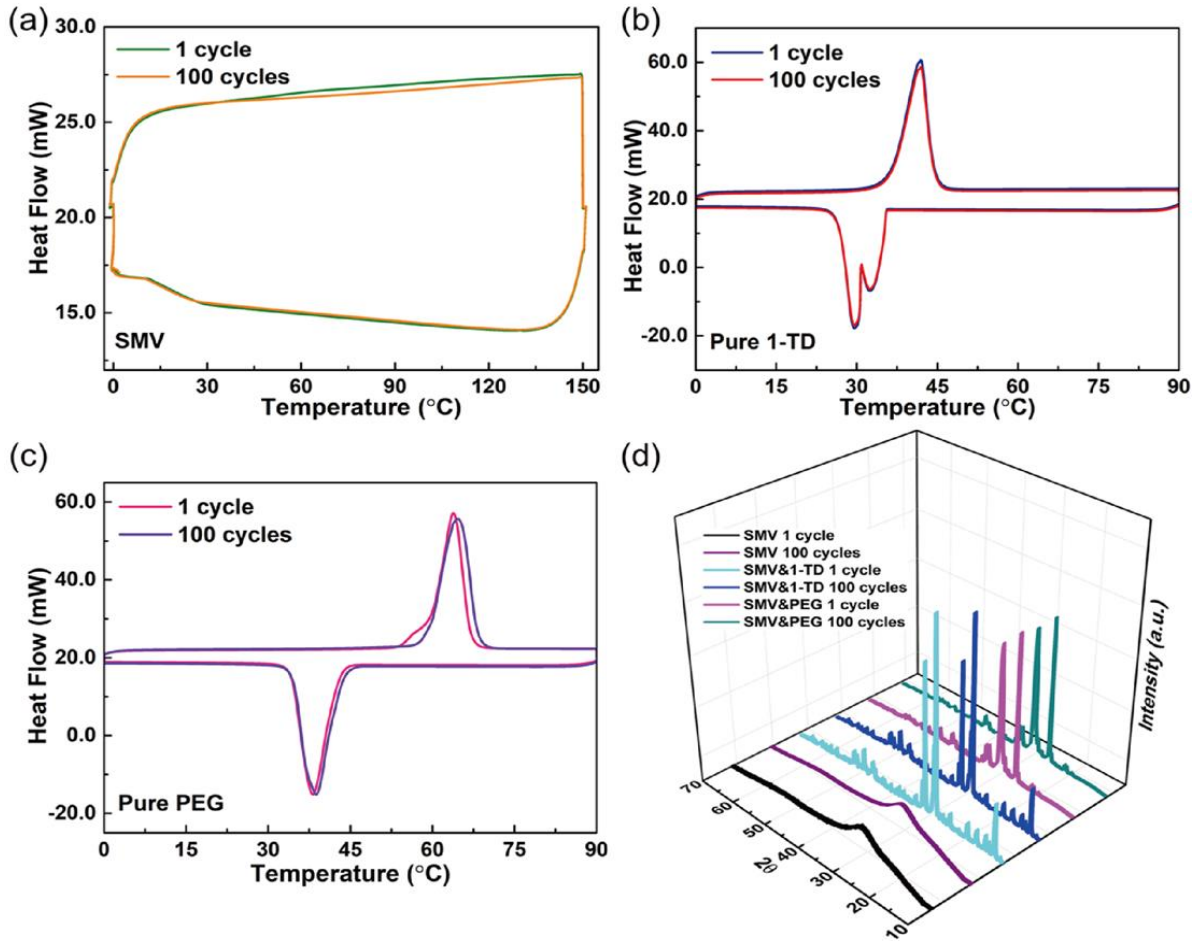

Fig. S13. DSC cycling results of (a) SMV, (b) pure -1TD, and (c) pure PEG. (d) XRD peaks after 100 cycles.

Table S2. DSC cycling results of SMV, pure 1-TD and PEG.

Samples	T_{mp}(°C)	ΔH_m(J/g)	T_{cp}(°C)	ΔH_c(J/g)
SMV 1 cycle	-	-	-	-
SMV 100 cycles	-	-	-	-
1-TD 1cycle	**41.12**	**223.40**	**31.25**	**220.78**
1-TD 100 cycles	**41.07**	**222.83**	**31.19**	**220.42**
PEG 1 cycle	**62.98**	**181.68**	**38.82**	**165.73**
PEG 100 cycles	**63.84**	**181.55**	**38.86**	**165.69**

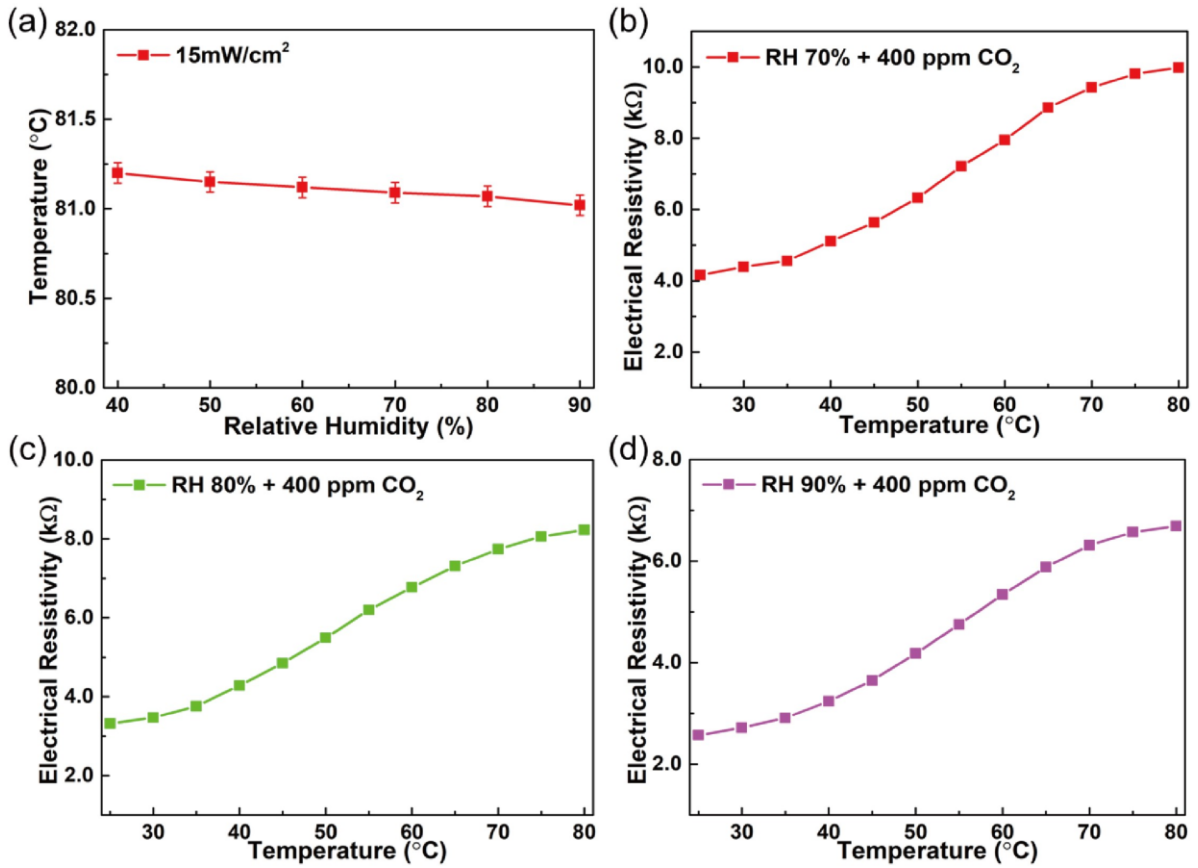

Fig. S14. (a) The final temperature with different RH at 15 mW/cm^2 solar light intensity. Electrical resistivity peaks of (b) RH 70% with initial 400 ppm CO_2 concentration, (c) RH 80% with initial 400 ppm CO_2 concentration, and (d) RH 90% with initial 400 ppm CO_2 concentration.

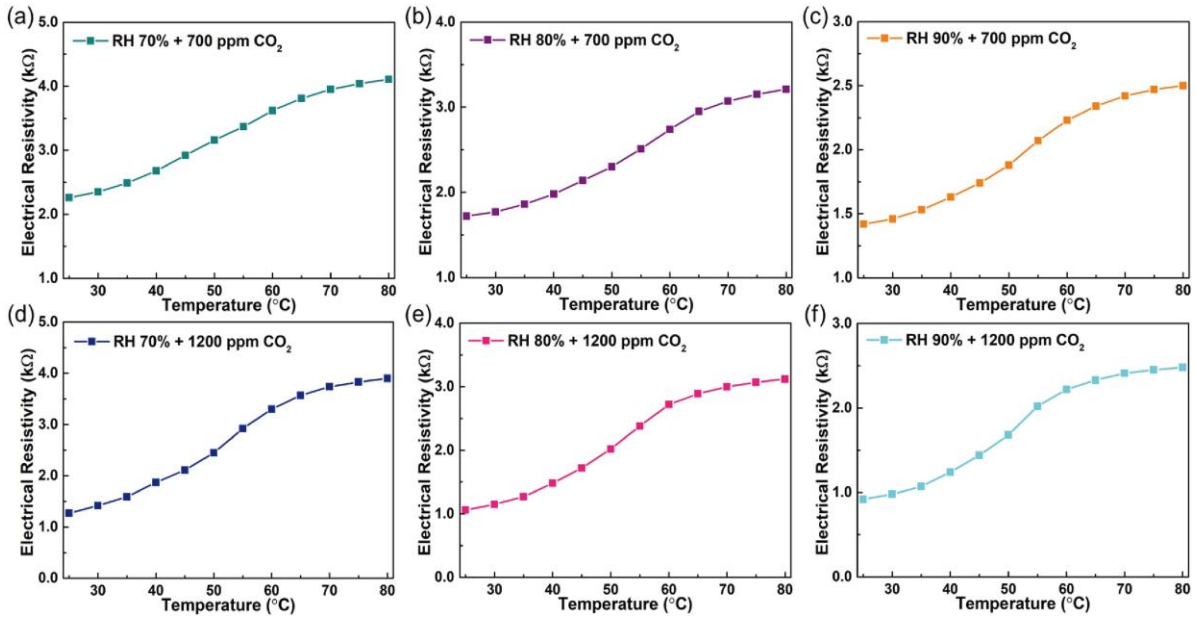

Fig. S15. Electrical resistivity peaks of (a) RH 70% with 700 ppm CO_2 concentration, (b) RH 80% with initial 700 ppm CO_2 concentration, (c) RH 90% with initial 700 ppm CO_2 concentration, (d) RH 70% with initial 1200 ppm CO_2 concentration, (e) RH 80% with initial 1200 ppm CO_2 concentration, and (f) RH 90% with initial 1200 ppm CO_2 concentration.

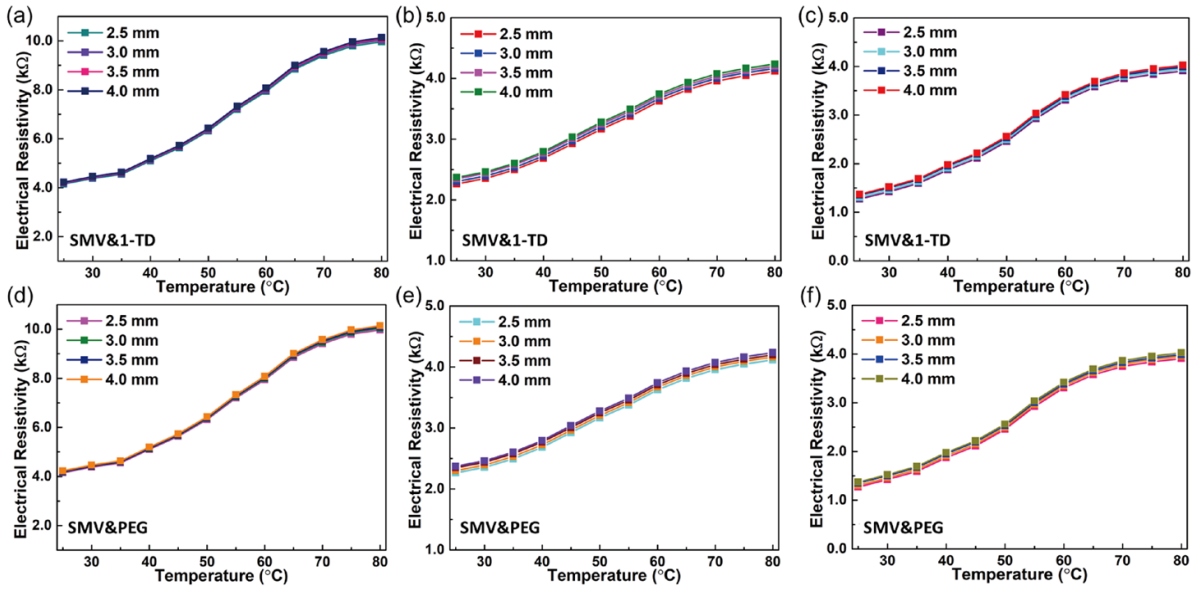

Fig. S16. The electrical resistivity at RH 70%, the different thickness of SMV supported 1-TD composite under (a) 400 ppm CO_2 concentration, (b) 700 ppm CO_2 concentration, (c) 1200 ppm CO_2 concentration. For the different thickness of SMV supported PEG composites under (d) 400 ppm CO_2 concentration, (e) 700 ppm CO_2 concentration, and (f) 1200 ppm CO_2 concentration.

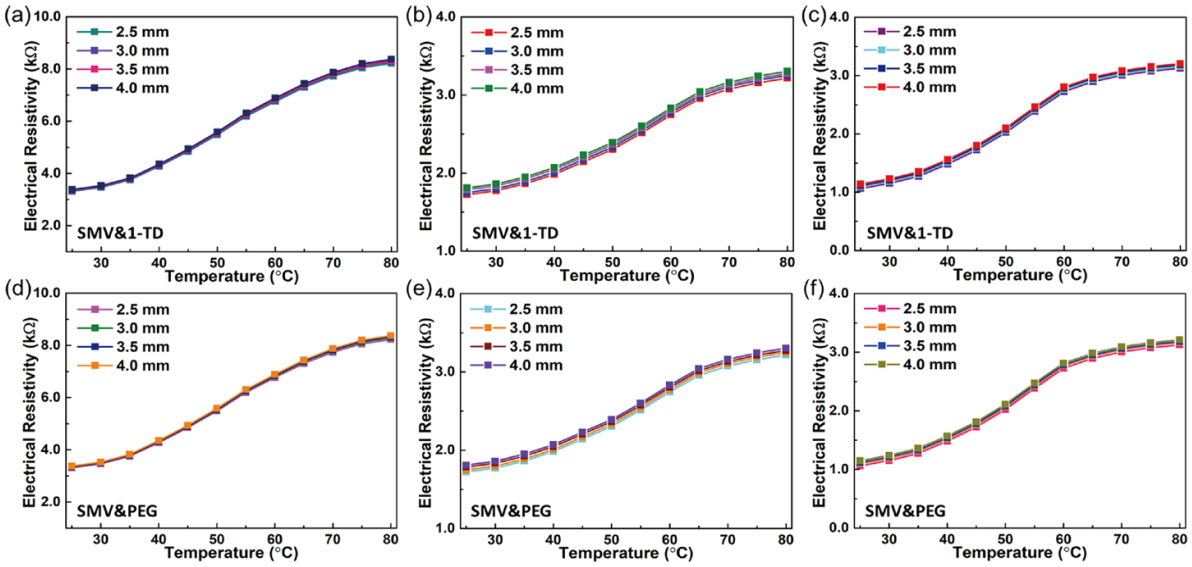

Fig. S17. The electrical resistivity at RH 80%, the different thickness of SMV supported 1-TD composite under (a) 400 ppm CO_2 concentration, (b) 700 ppm CO_2 concentration, (c) 1200 ppm CO_2 concentration. For the different thickness of SMV supported PEG composites under (d) 400 ppm CO_2 concentration, (e) 700 ppm CO_2 concentration, and (f) 1200 ppm CO_2 concentration.

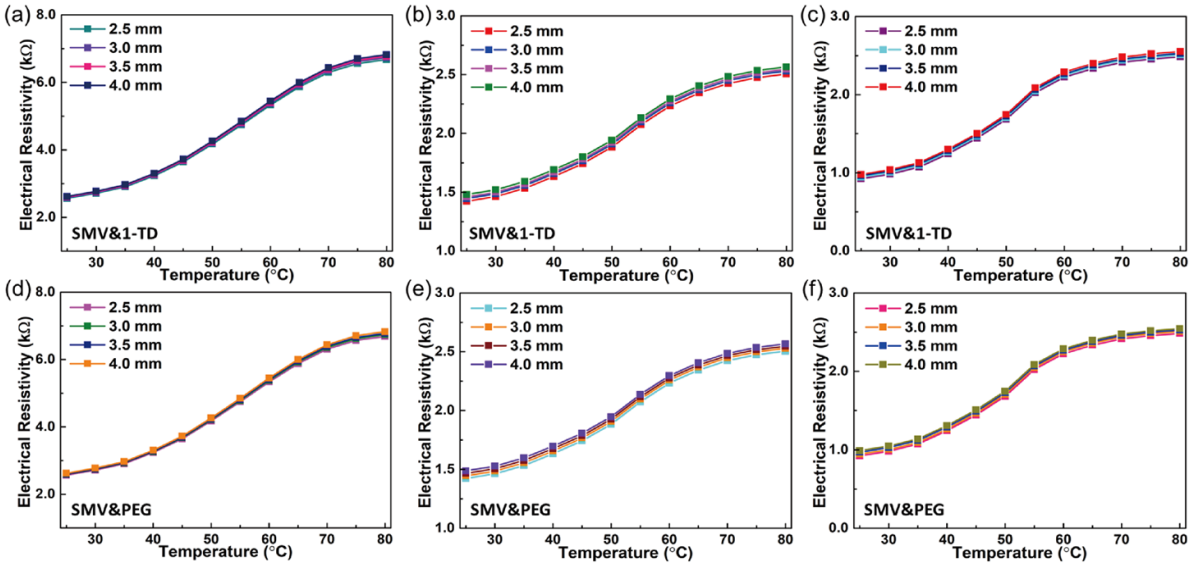

Fig. S18. The electrical resistivity at RH 90%, the different thickness of SMV supported 1-TD composite under (a) 400 ppm CO_2 concentration, (b) 700 ppm CO_2 concentration, (c) 1200 ppm CO_2 concentration. For the different thickness of SMV supported PEG composites under (d) 400 ppm CO_2 concentration, (e) 700 ppm CO_2 concentration, and (f) 1200 ppm CO_2 concentration.

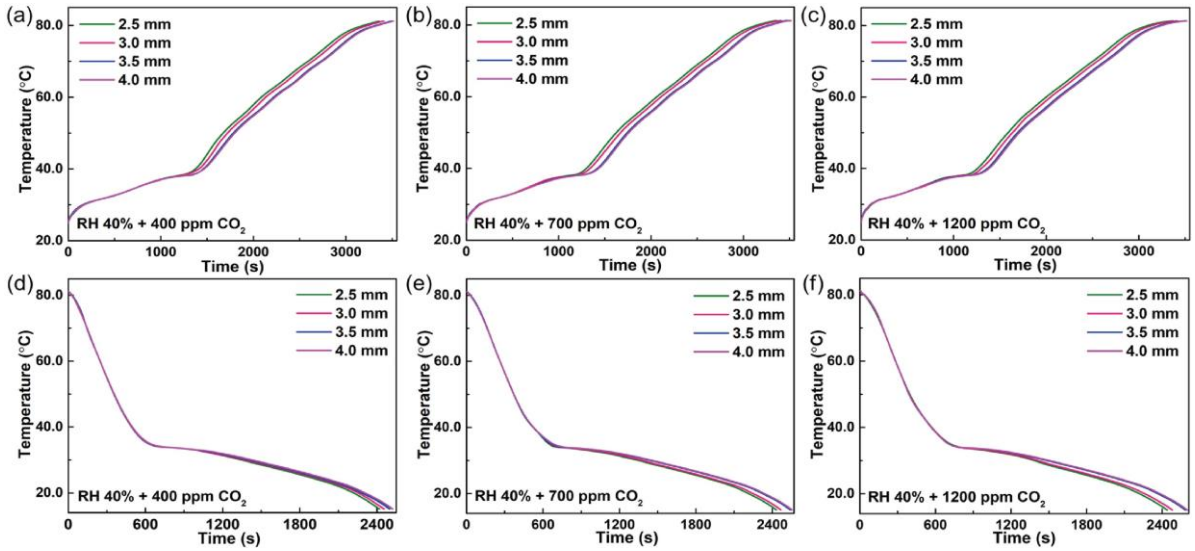

Fig. S19. The temperature peaks of different thickness of SMV supported 1-TD composites, the light-on process at (a) RH 40% with 400 ppm CO_2 concentration, (b) RH 40% with 700 ppm CO_2 concentration, (c) RH 40% with 1200 ppm CO_2 concentration. For light-off process, (d) RH 40% with 400 ppm CO_2 concentration, (e) RH 40% with 700 ppm CO_2 concentration, (f) RH 40% with 1200 ppm CO_2 concentration.

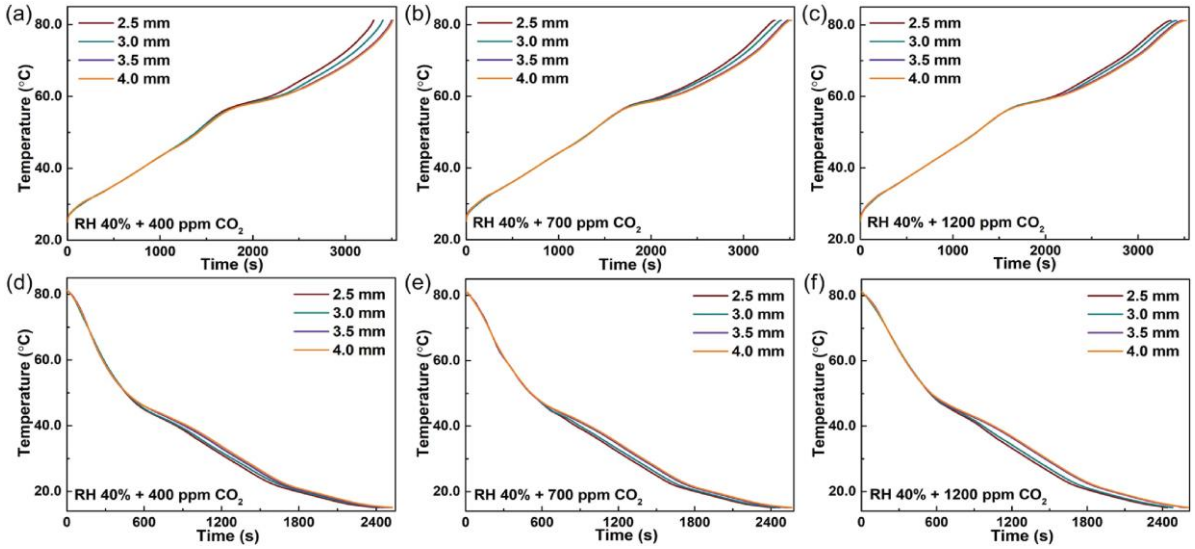

Fig. S20. The temperature peaks of different thickness of SMV supported PEG composites, the light-on process at (a) RH 40% with 400 ppm CO_2 concentration, (b) RH 40% with 700 ppm CO_2 concentration, (c) RH 40% with 1200 ppm CO_2 concentration. For light-off process, (d) RH 40% with 400 ppm CO_2 concentration, (e) RH 40% with 700 ppm CO_2 concentration, (f) RH 40% with 1200 ppm CO_2 concentration.

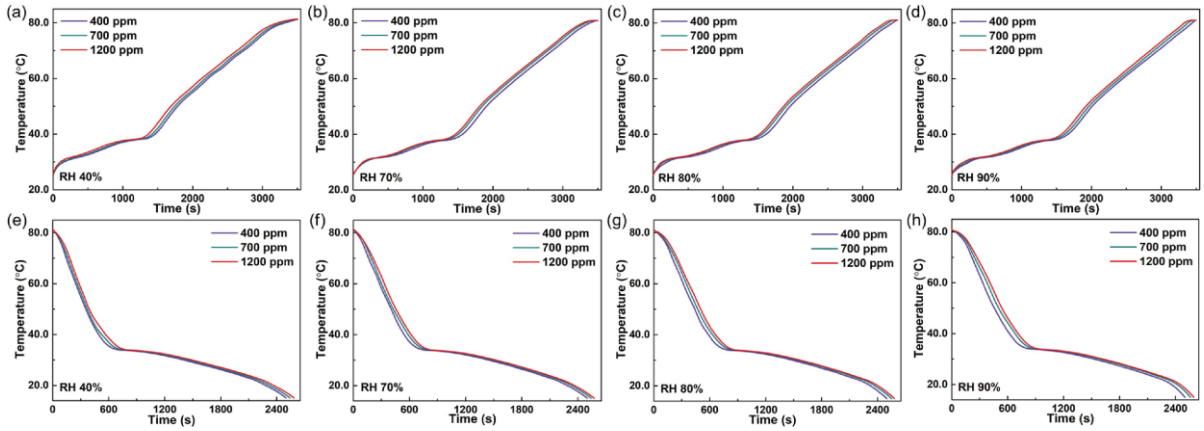

Fig. S21. The temperature peaks of 3.5 mm height SMV supported 1-TD composite, the light-on process at (a) RH 40% with different CO_2 concentration, (b) RH 70% with different CO_2 concentration, (c) RH 80% with different CO_2 concentration, and (d) RH 90% with different CO_2 concentration. For light-off process, (e) RH 40% with different CO_2 concentration, (f) RH 70% with different CO_2 concentration, (g) RH 80% with different CO_2 concentration, and (h) RH 90% with different CO_2 concentration.

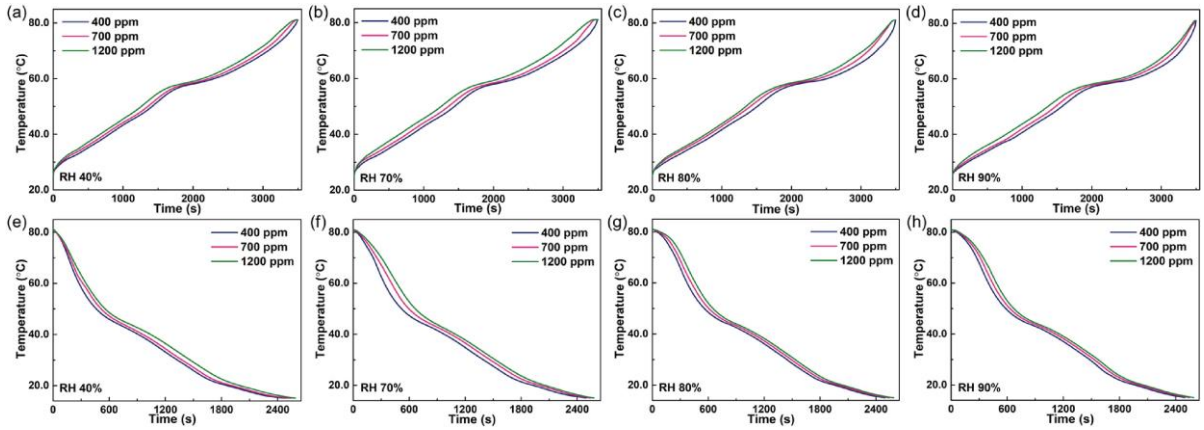

Fig. S22. The temperature peaks of 3.5 mm height SMV supported PEG composite, the light-on process at (a) RH 40% with different CO_2 concentration, (b) RH 70% with different CO_2 concentration, (c) RH 80% with different CO_2 concentration, and (d) RH 90% with different CO_2 concentration. For light-off process, (e) RH 40% with different CO_2 concentration, (f) RH 70% with different CO_2 concentration, (g) RH 80% with different CO_2 concentration, and (h) RH 90% with different CO_2 concentration.

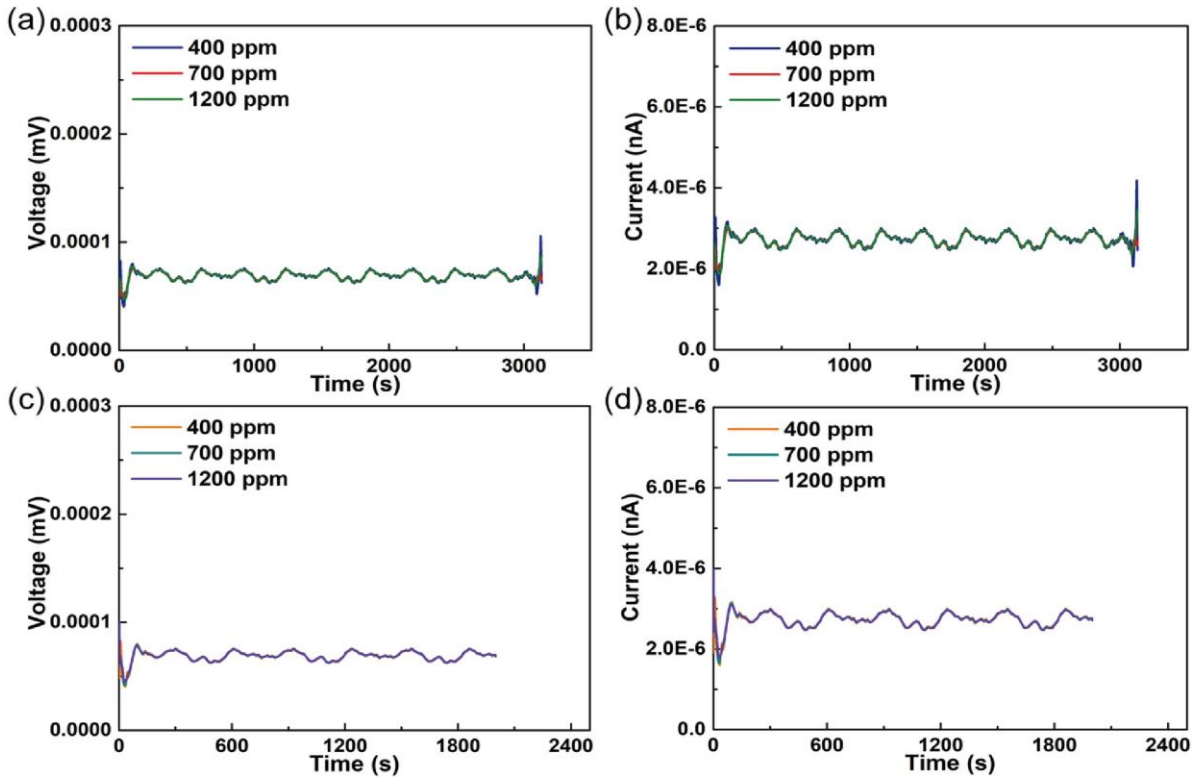

Fig. S23. The assembly made of RH 40% SMV supported 1-TD and RH 40% SMV supported PEG, the light-on process with (a) voltage at different CO_2 concentration (b) current at different CO_2 concentration. For light-off process, (c) voltage at different CO_2 concentration (d) current at different CO_2 concentration.

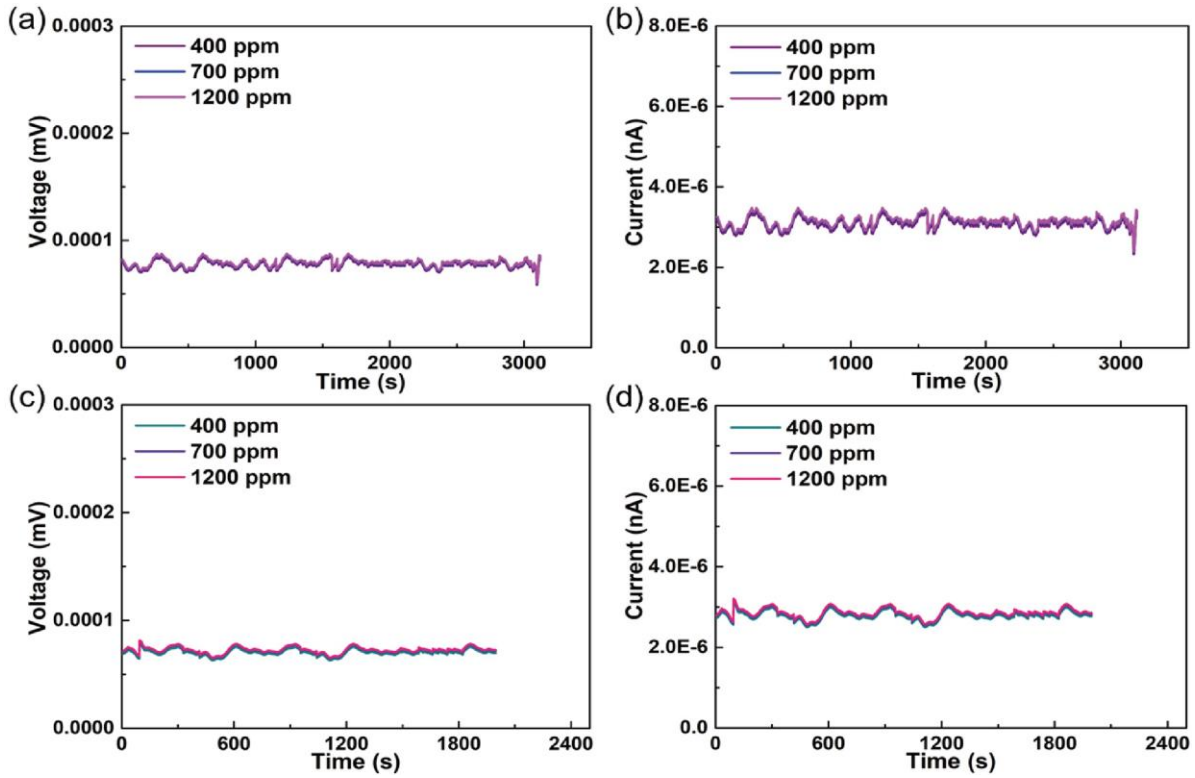

Fig. S24. The assembly made of RH 40% SMV supported 1-TD and RH 70% SMV supported PEG, the light-on process with (a) voltage at different CO_2 concentration (b) current at different CO_2 concentration. For light-off process, (c) voltage at different CO_2 concentration (d) current at different CO_2 concentration.

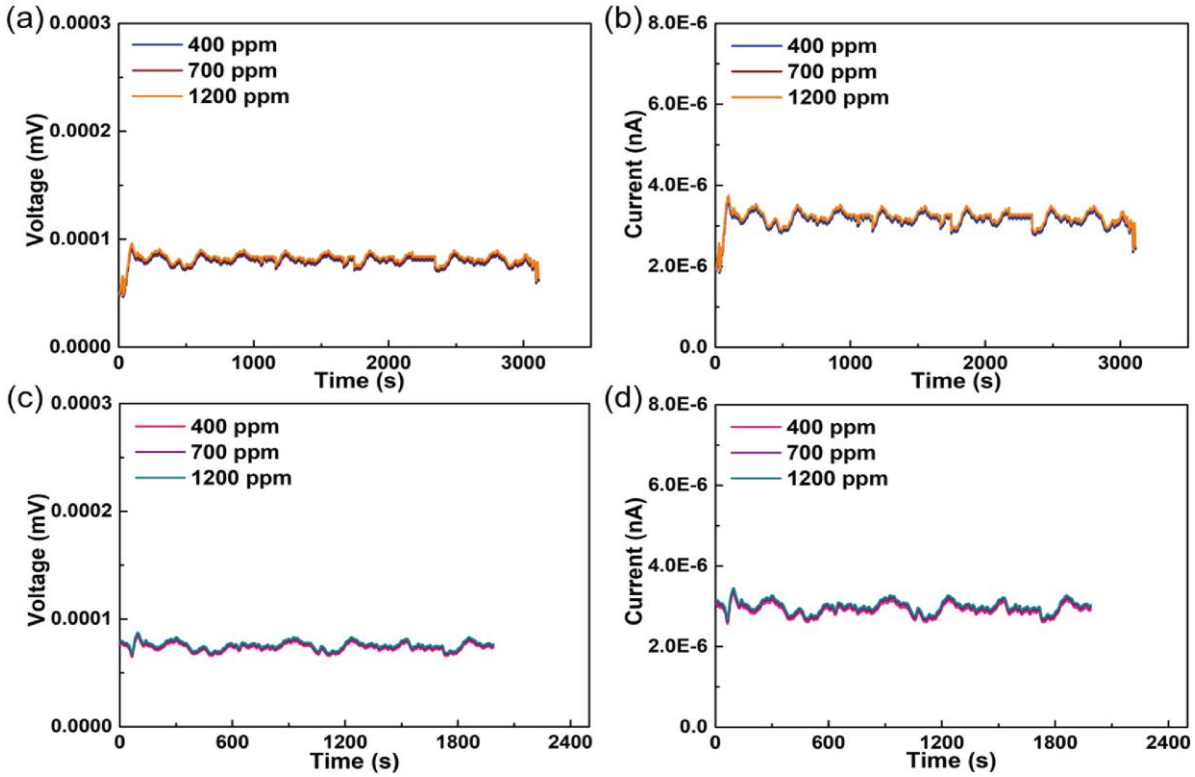

Fig. S25. The assembly made of RH 70% SMV supported 1-TD and RH 40% SMV supported PEG, the light-on process with (a) voltage at different CO_2 concentration (b) current at different CO_2 concentration. For light-off process, (c) voltage at different CO_2 concentration (d) current at different CO_2 concentration.

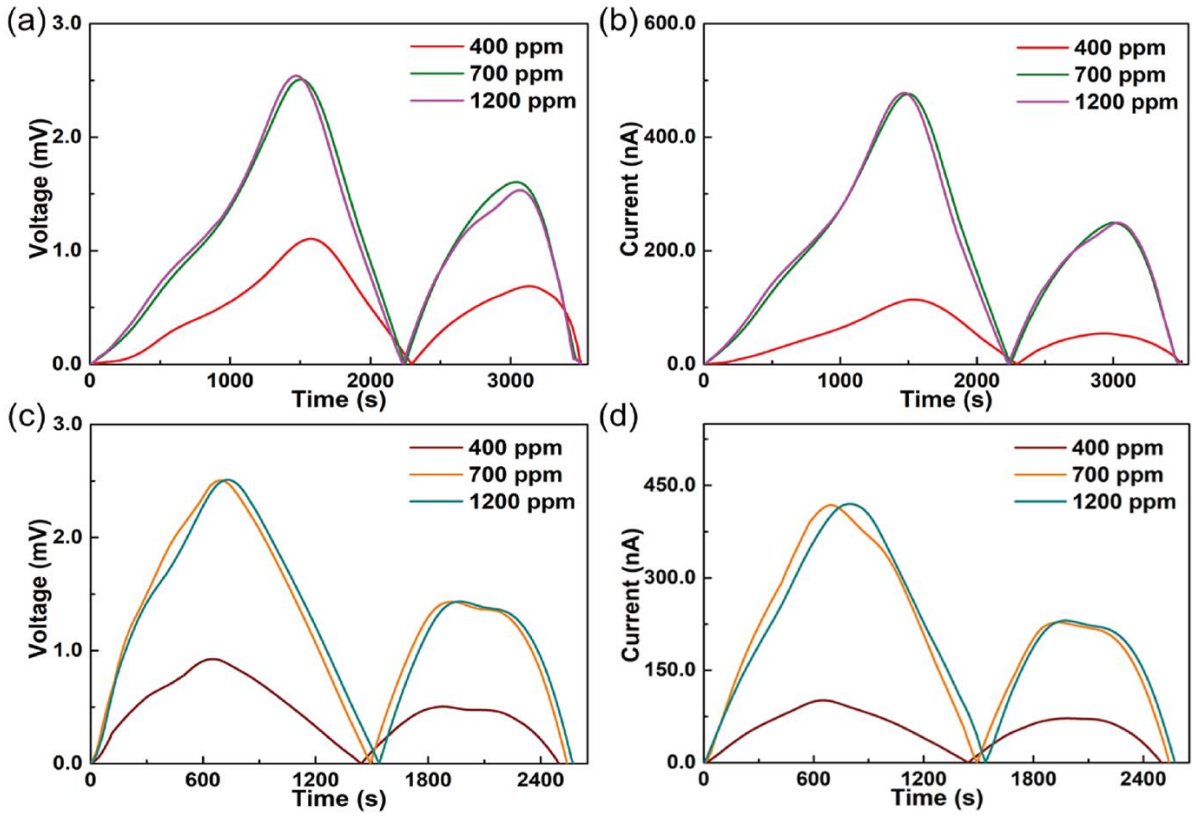

Fig. S26. The assembly made of RH 70% SMV supported 1-TD and RH 80% SMV supported PEG, the light-on process with (a) voltage at different CO_2 concentration (b) current at different CO_2 concentration. For light-off process, (c) voltage at different CO_2 concentration (d) current at different CO_2 concentration.

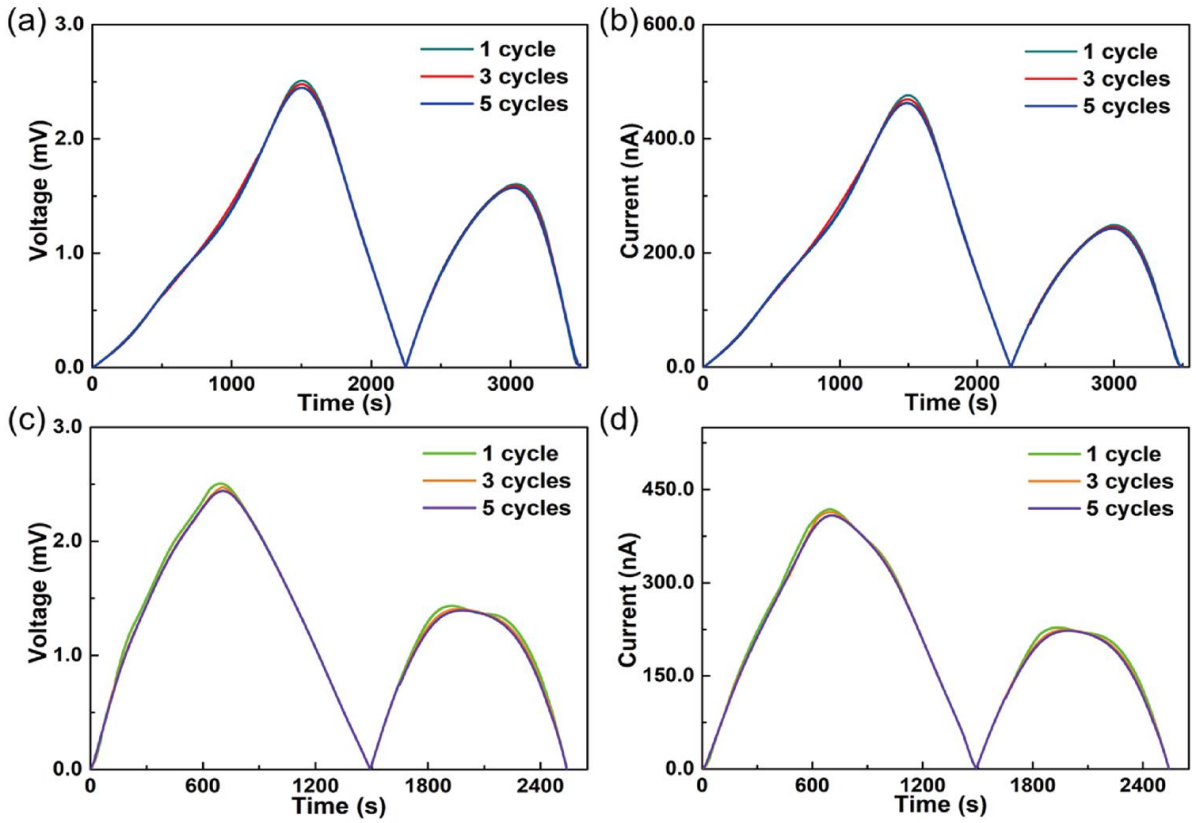

Fig. S27. Long-term durability of the assembly made of RH 70% SMV supported 1-TD and RH 80% SMV supported PEG under the 700 ppm CO_2 concentration (a) Output voltage and (b) output current up to 5 cycles upon light-on process. (c) Output voltage and (d) output current up to 5 cycles upon light-off process.

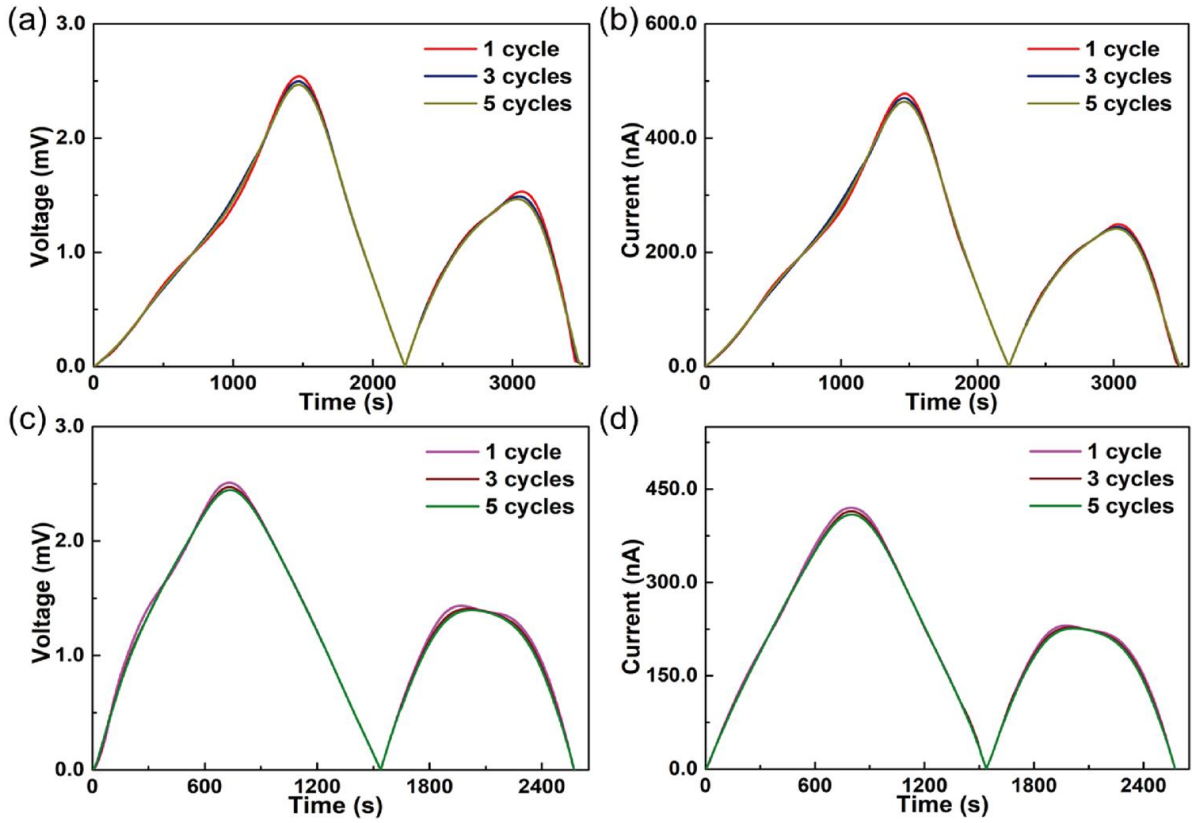

Fig. S28. Long-term durability of the assembly made of RH 70% SMV supported 1-TD and RH 80% SMV supported PEG under the 1200 ppm CO_2 concentration (a) Output voltage and (b) output current up to 5 cycles upon light-on process. (c) Output voltage and (d) output current up to 5 cycles upon light-off process.

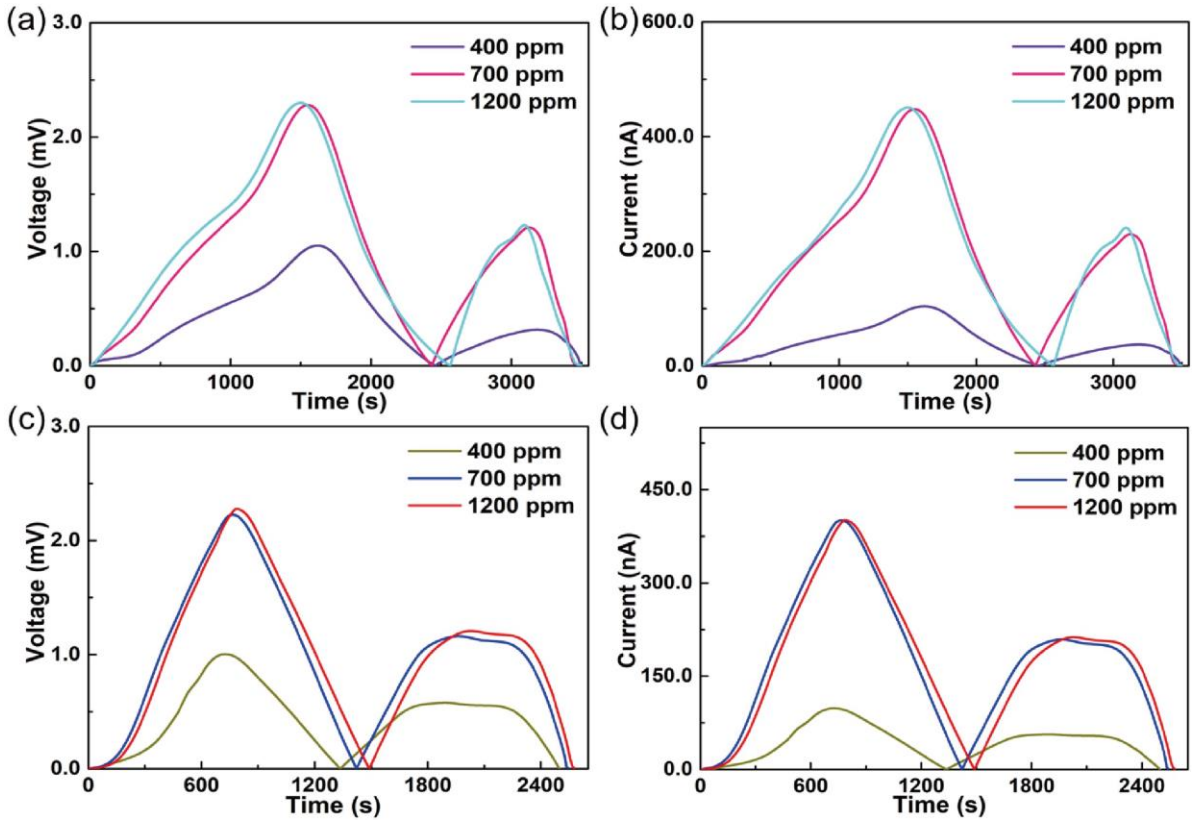

Fig. S29. The assembly made of RH 80% SMV supported 1-TD and RH 70% SMV supported PEG, the light-on process with (a) voltage at different CO_2 concentration (b) current at different CO_2 concentration. For light-off process, (c) voltage at different CO_2 concentration (d) current at different CO_2 concentration.

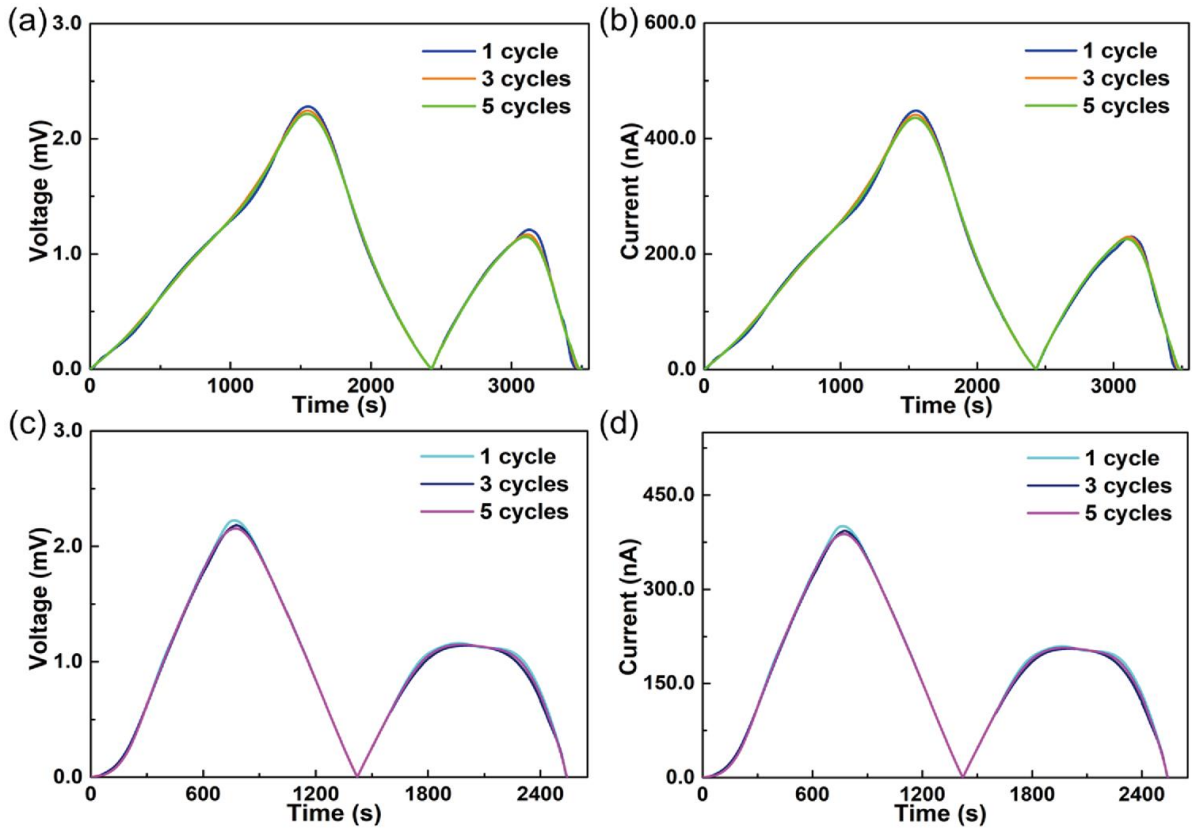

Fig. S30. Long-term durability of the assembly made of RH 80% SMV supported 1-TD and RH 70% SMV supported PEG under the 700 ppm CO_2 concentration (a) Output voltage and (b) output current up to 5 cycles upon light-on process. (c) Output voltage and (d) output current up to 5 cycles upon light-off process.

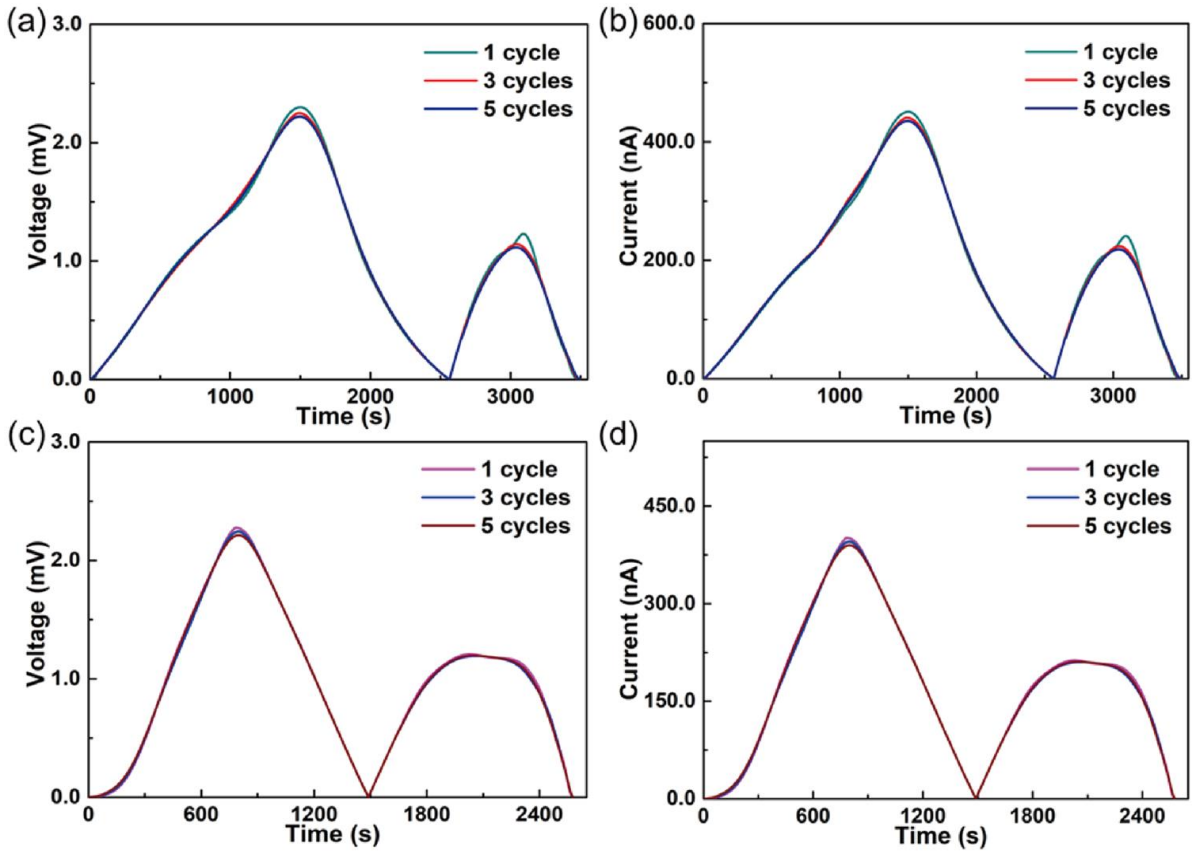

Fig. S31. Long-term durability of the assembly made of RH 80% SMV supported 1-TD and RH 70% SMV supported PEG under the 1200 ppm CO_2 concentration (a) Output voltage and (b) output current up to 5 cycles upon light-on process. (c) Output voltage and (d) output current up to 5 cycles upon light-off process.

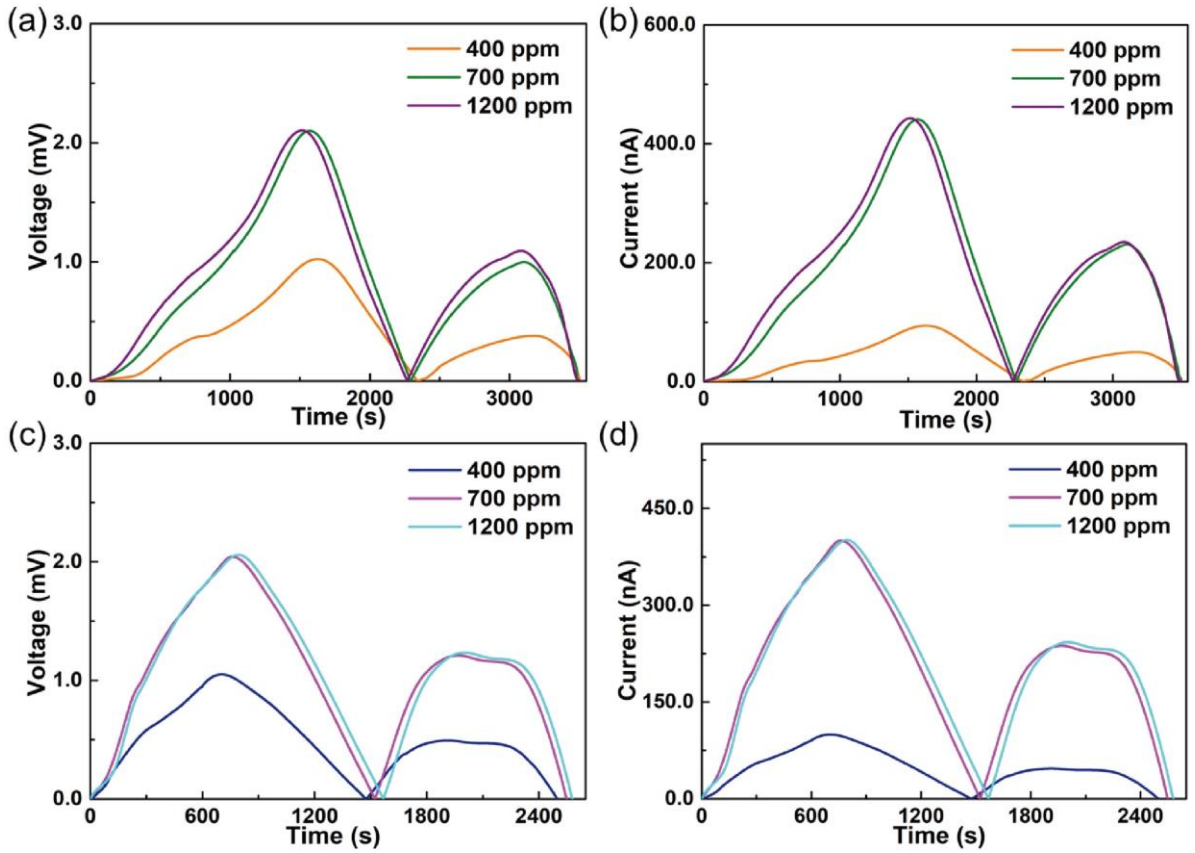

Fig. S32. The assembly made of RH 80% SMV supported 1-TD and RH 90% SMV supported PEG, the light-on process with (a) voltage at different CO_2 concentration (b) current at different CO_2 concentration. For light-off process, (c) voltage at different CO_2 concentration (d) current at different CO_2 concentration.

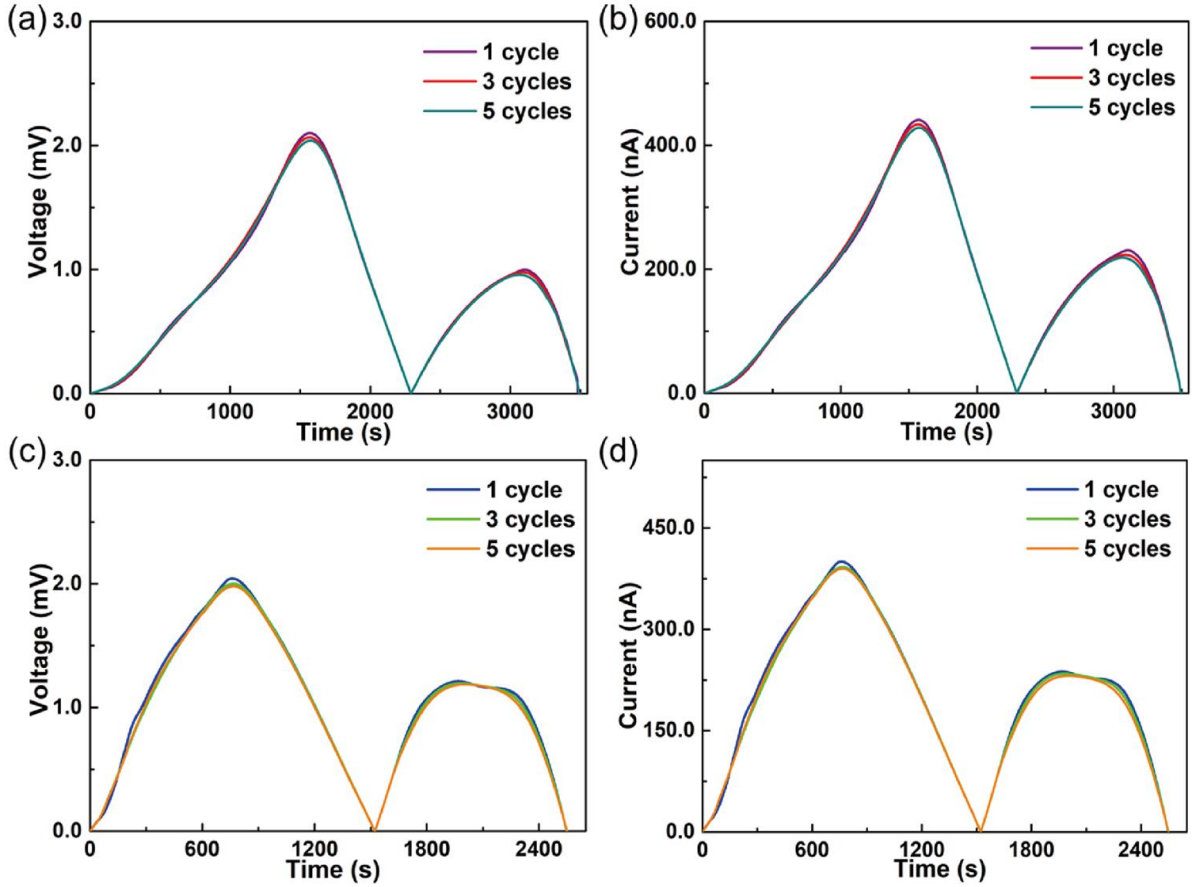

Fig. S33. Long-term durability of the assembly made of RH 80% SMV supported 1-TD and RH 90% SMV supported PEG under the 700 ppm CO_2 concentration (a) Output voltage and (b) output current up to 5 cycles upon light-on process. (c) Output voltage and (d) output current up to 5 cycles upon light-off process.

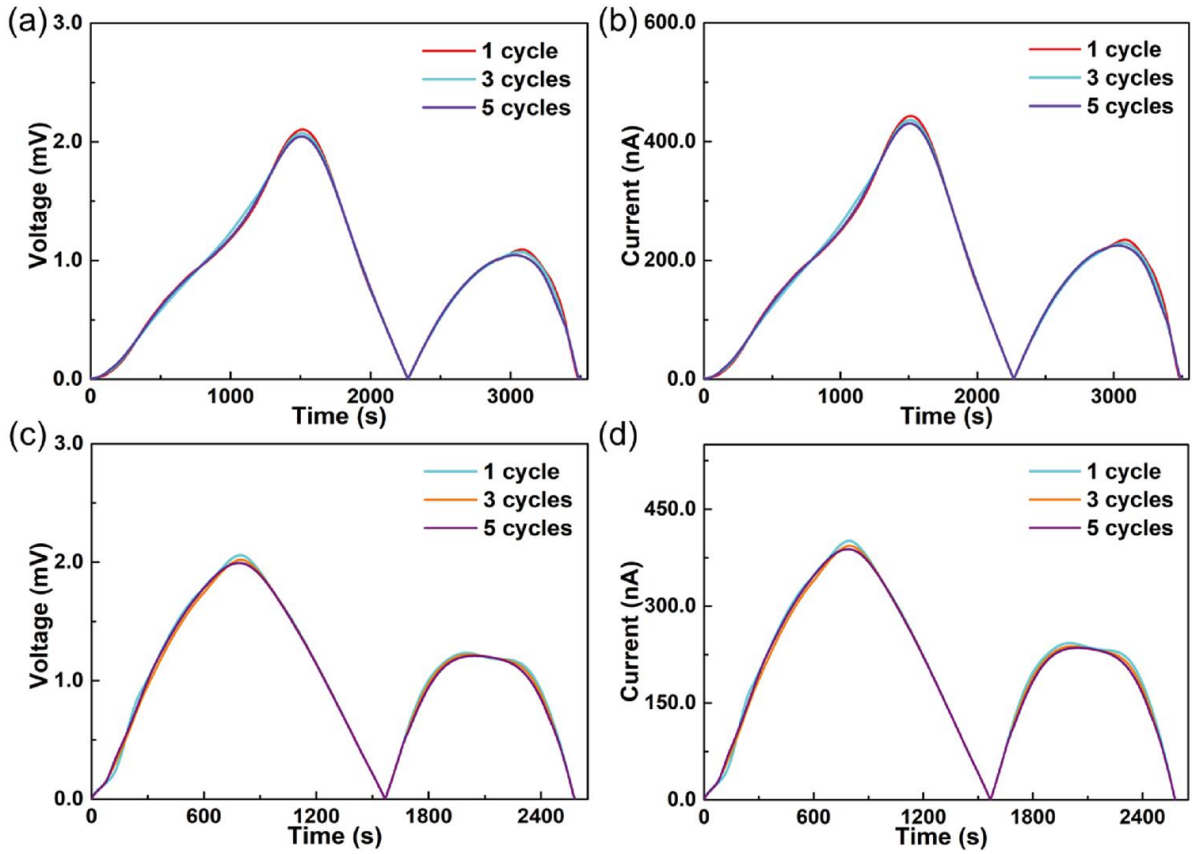

Fig. S34. Long-term durability of the assembly made of RH 80% SMV supported 1-TD and RH 90% SMV supported PEG under the 1200 ppm CO_2 concentration (a) Output voltage and (b) output current up to 5 cycles upon light-on process. (c) Output voltage and (d) output current up to 5 cycles upon light-off process.

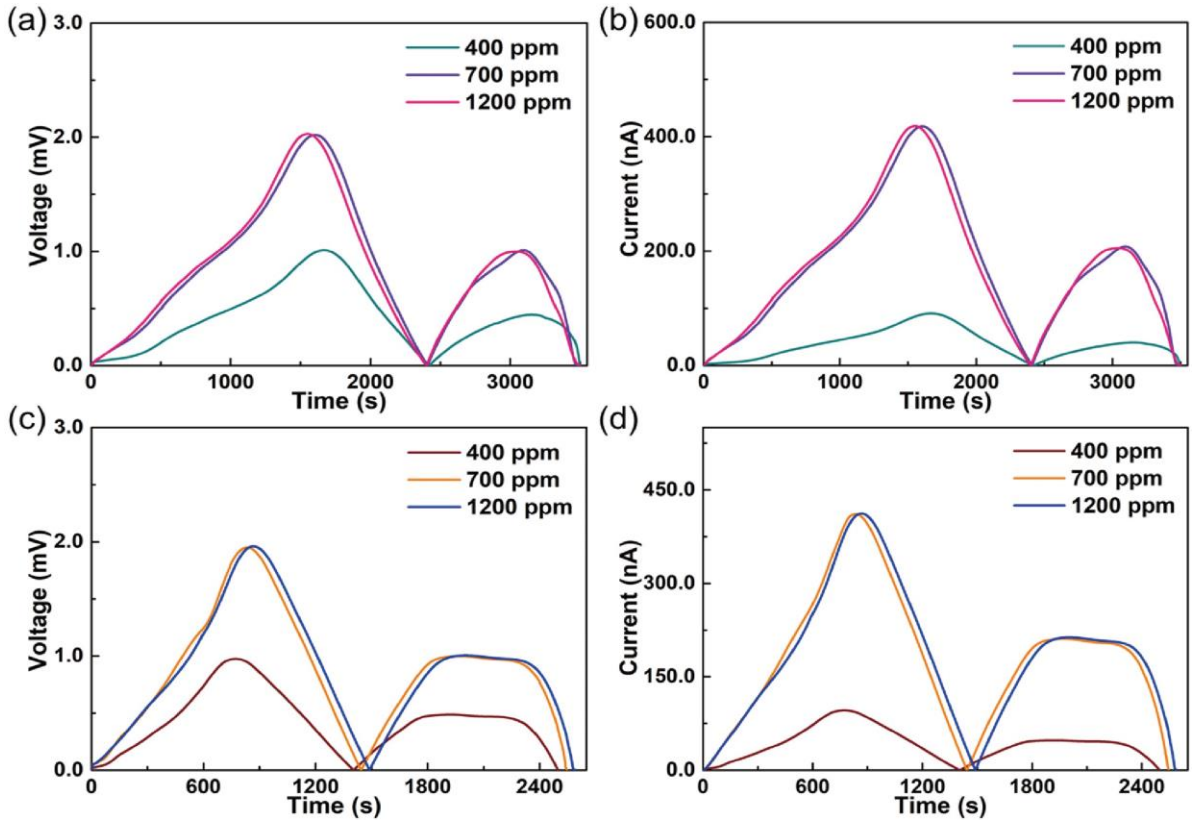

Fig. S35. The assembly made of RH 90% SMV supported 1-TD and RH 80% SMV supported PEG, the light-on process with (a) voltage at different CO_2 concentration (b) current at different CO_2 concentration. For light-off process, (c) voltage at different CO_2 concentration (d) current at different CO_2 concentration.

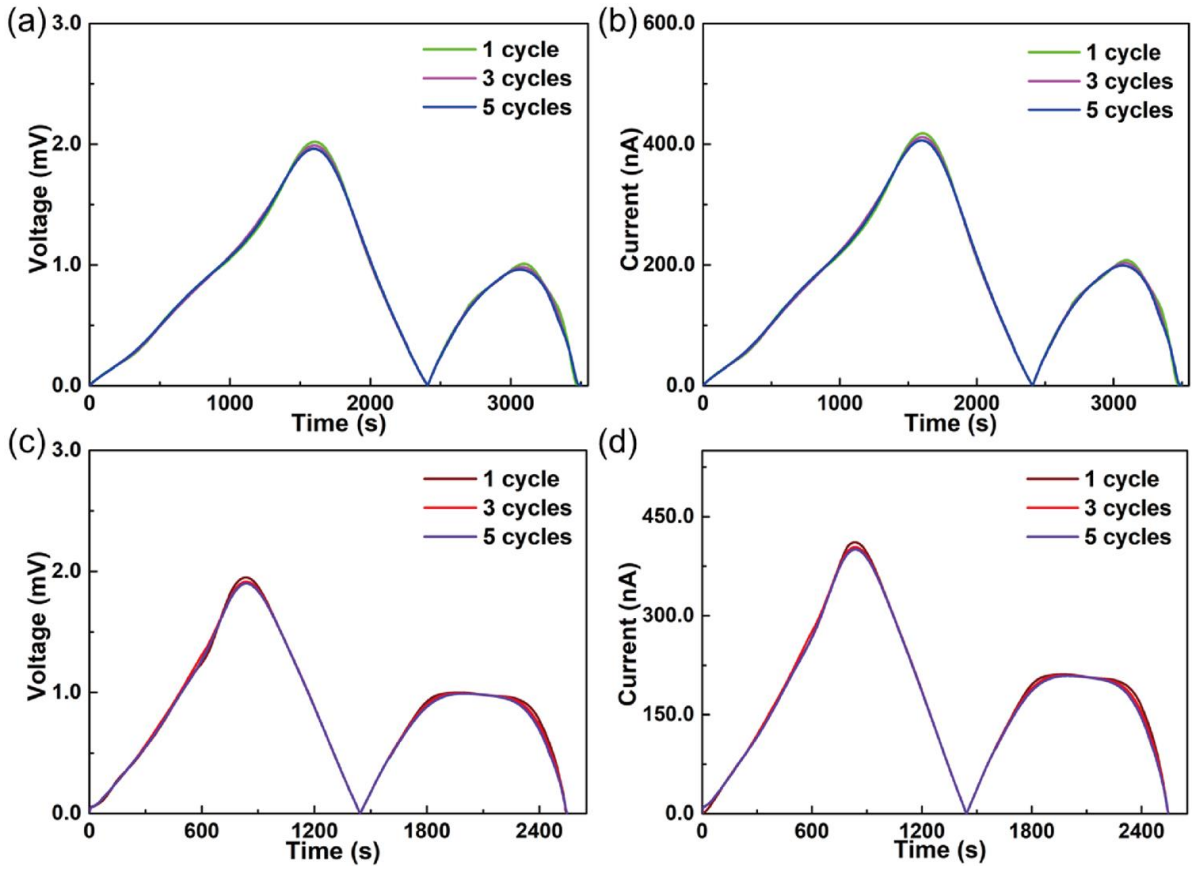

Fig. S36. Long-term durability of the assembly made of RH 90% SMV supported 1-TD and RH 80% SMV supported PEG under the 700 ppm CO_2 concentration (a) Output voltage and (b) output current up to 5 cycles upon light-on process. (c) Output voltage and (d) output current up to 5 cycles upon light-off process.

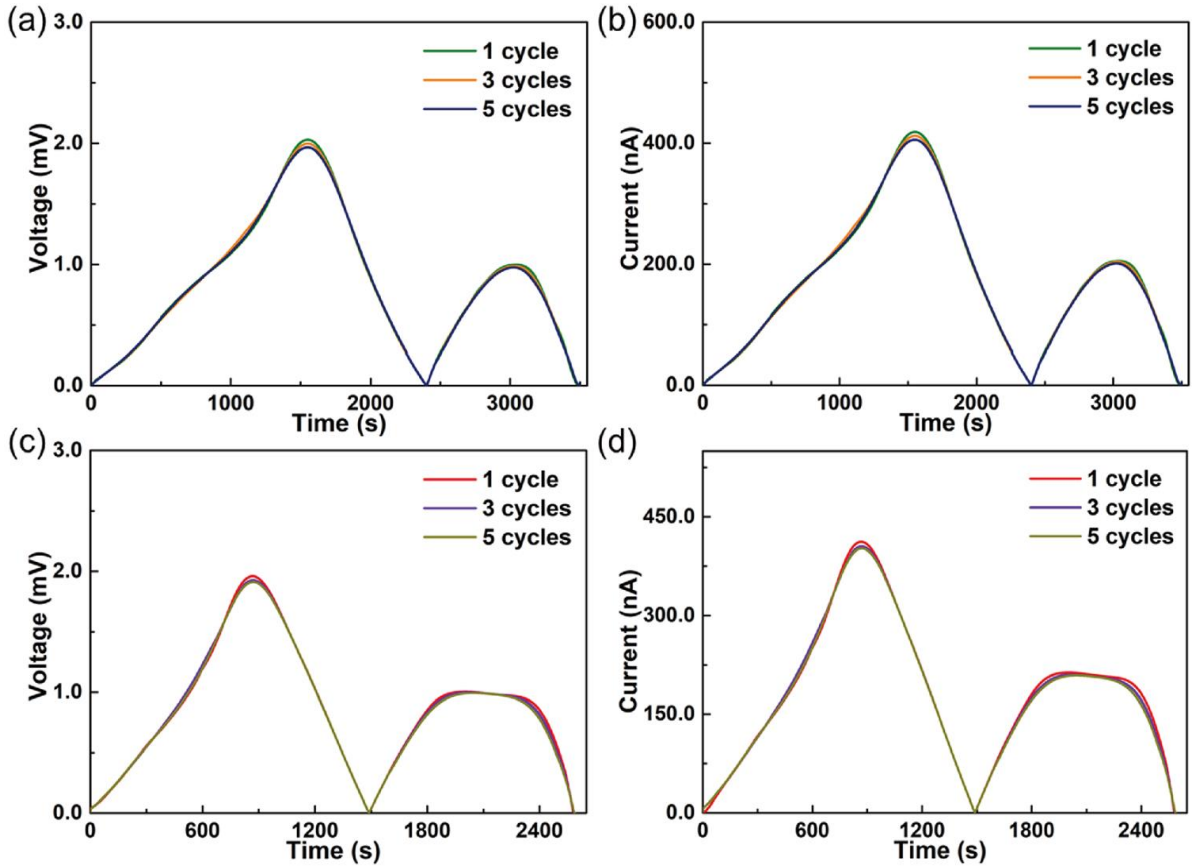

Fig. S37. Long-term durability of the assembly made of RH 90% SMV supported 1-TD and RH 80% SMV supported PEG under the 1200 ppm CO_2 concentration (a) Output voltage and (b) output current up to 5 cycles upon light-on process. (c) Output voltage and (d) output current up to 5 cycles upon light-off process.

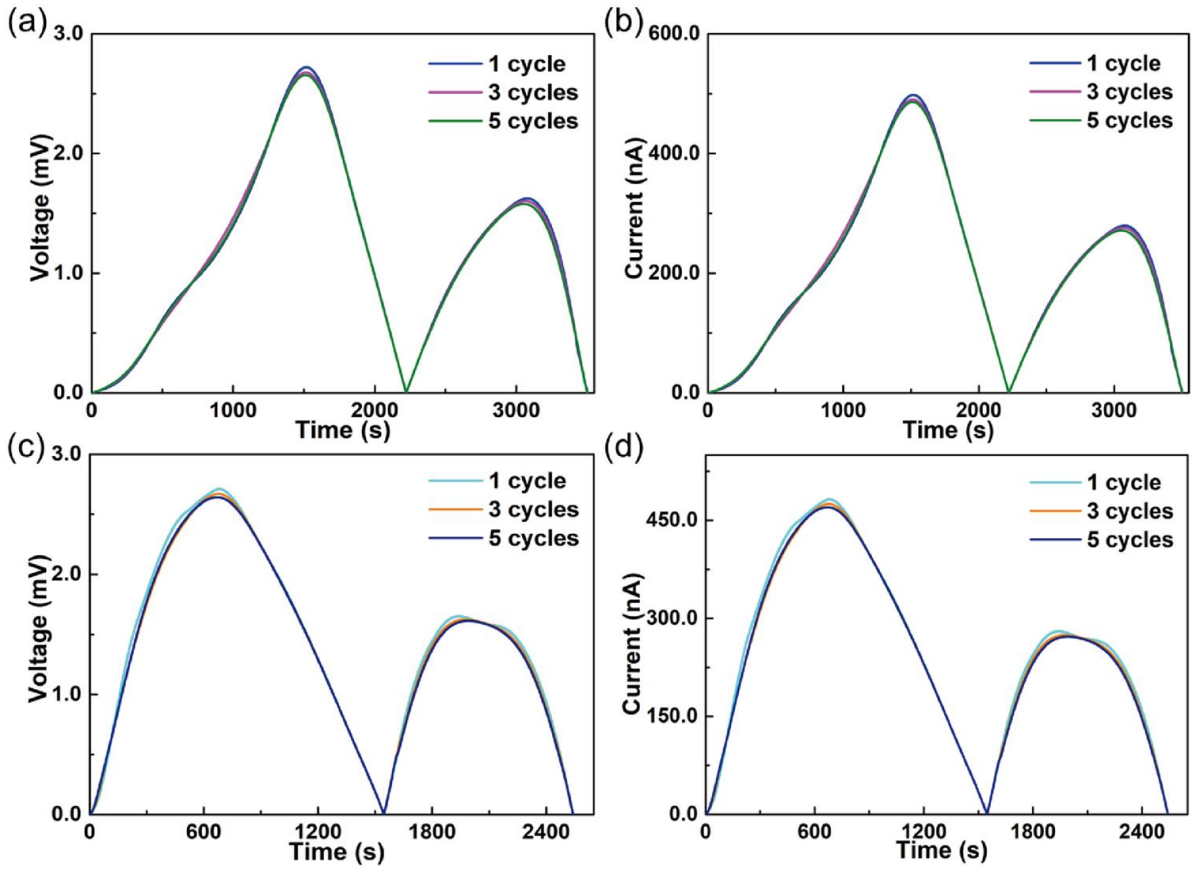

Fig. S38. Long-term durability of the assembly made of RH 70% SMV supported 1-TD and RH 90% SMV supported PEG under the 700 ppm CO_2 concentration (a) Output voltage and (b) output current up to 5 cycles upon light-on process. (c) Output voltage and (d) output current up to 5 cycles upon light-off process.

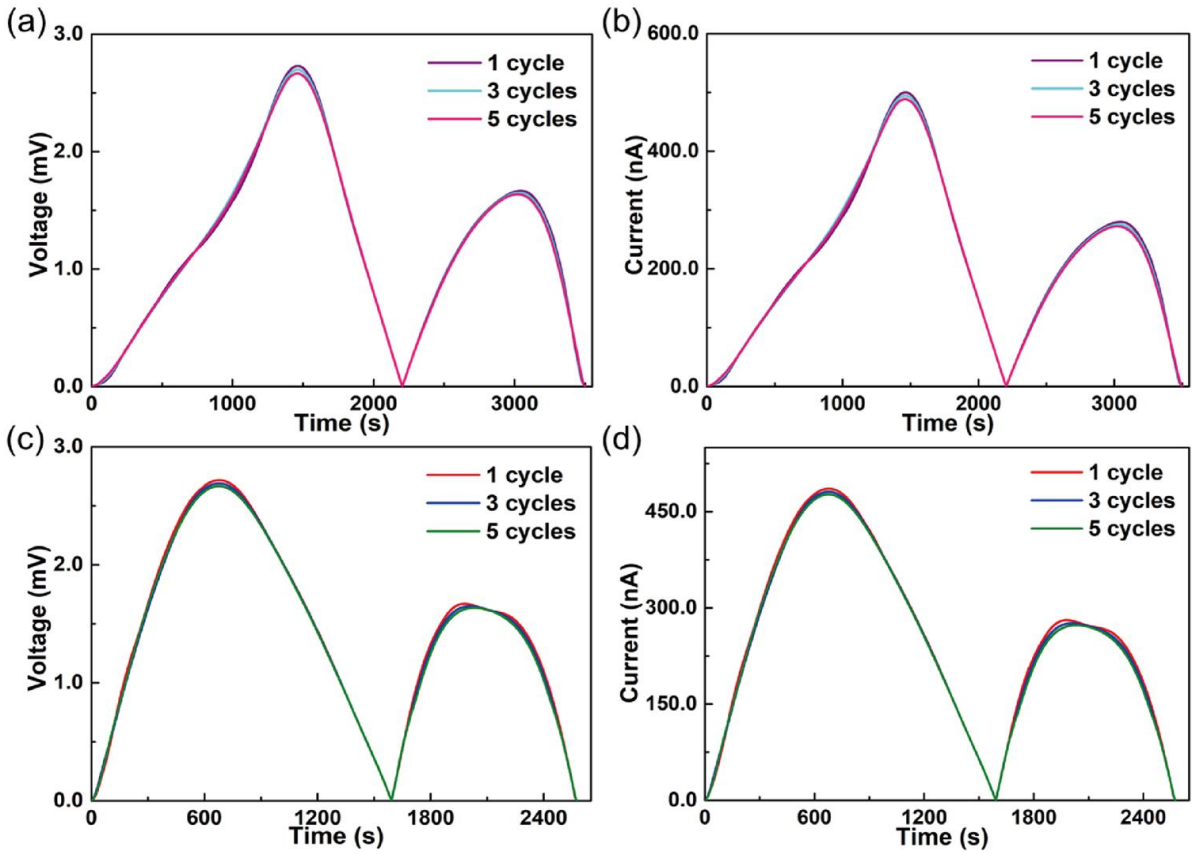

Fig. S39. Long-term durability of the assembly made of RH 70% SMV supported 1-TD and RH 90% SMV supported PEG under the 1200 ppm CO_2 concentration (a) Output voltage and (b) output current up to 5 cycles upon light-on process. (c) Output voltage and (d) output current up to 5 cycles upon light-off process.

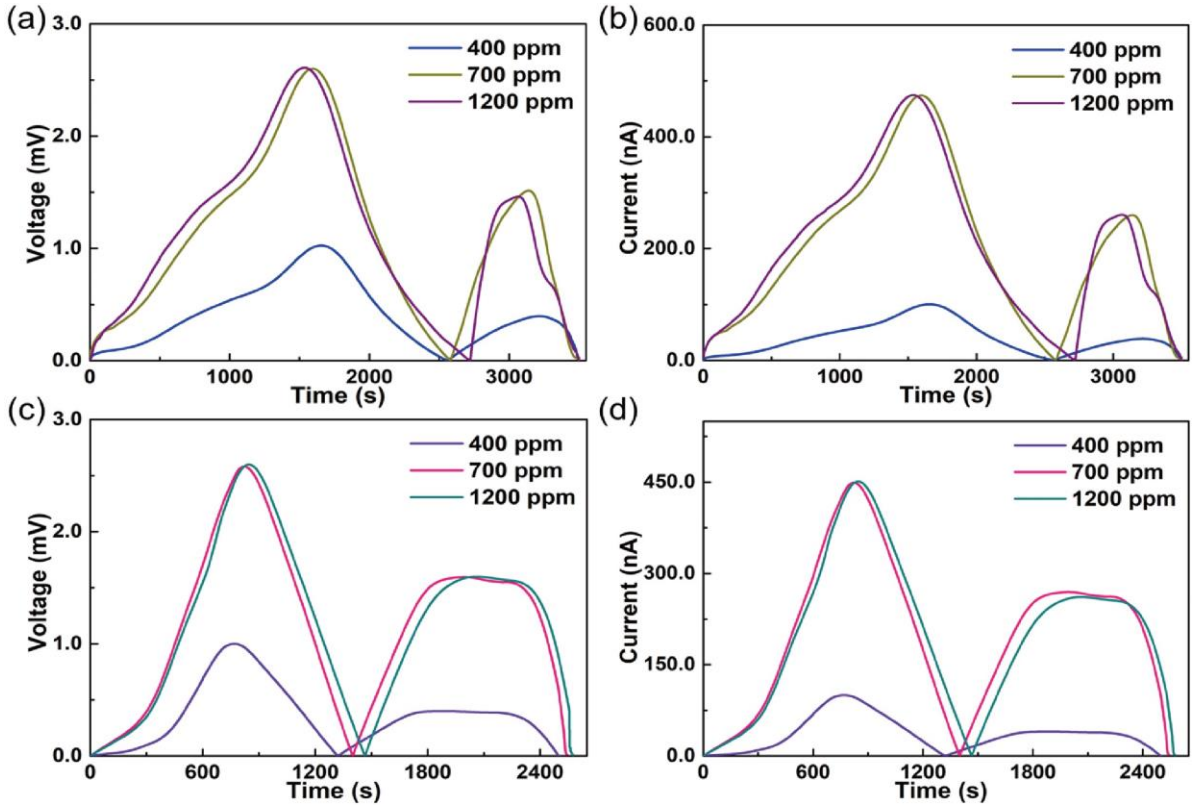

Fig. S40. The assembly made of RH 90% SMV supported 1-TD and RH 70% SMV supported PEG, the light-on process with (a) voltage at different CO_2 concentration (b) current at different CO_2 concentration. For light-off process, (c) voltage at different CO_2 concentration (d) current at different CO_2 concentration.

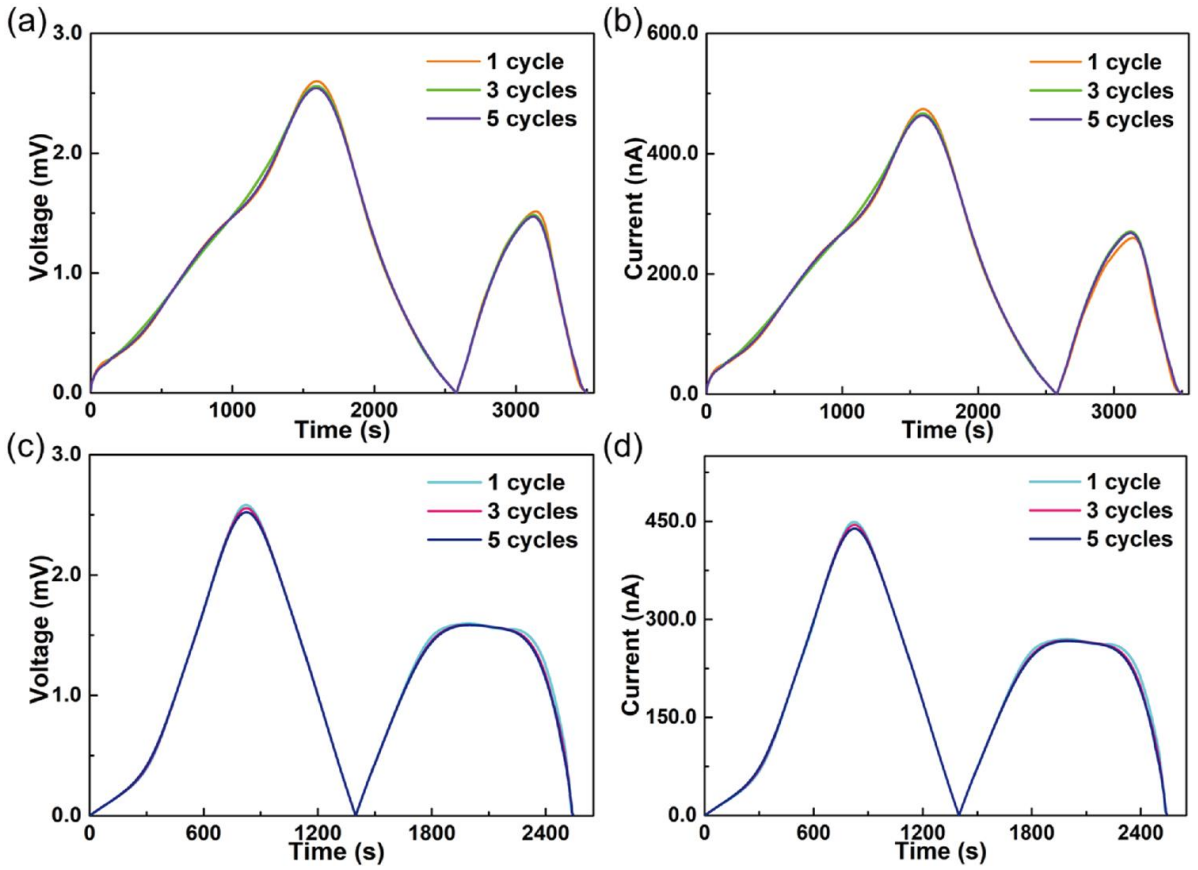

Fig. S41. Long-term durability of the assembly made of RH 90% SMV supported 1-TD and RH 70% SMV supported PEG under the 700 ppm CO_2 concentration (a) Output voltage and (b) output current up to 5 cycles upon light-on process. (c) Output voltage and (d) output current up to 5 cycles upon light-off process.

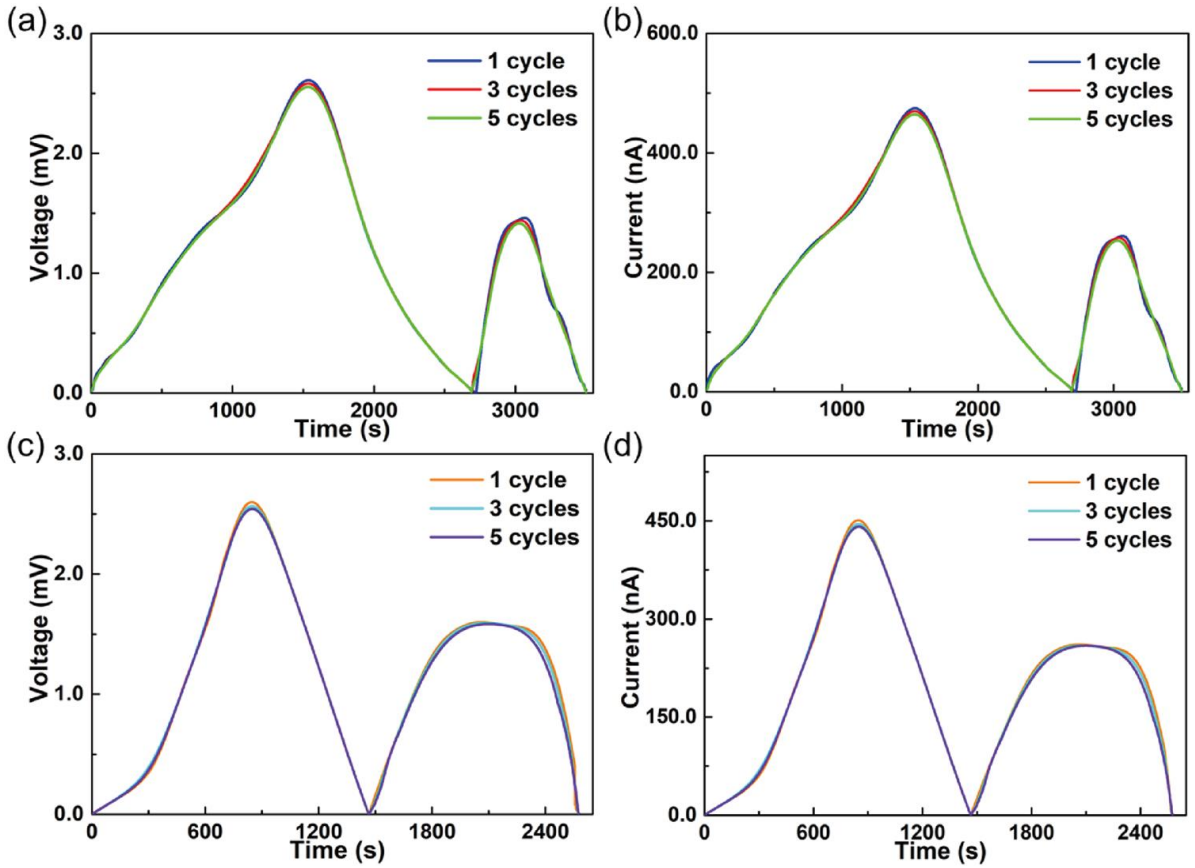

Fig. S42. Long-term durability of the assembly made of RH 90% SMV supported 1-TD and RH 70% SMV supported PEG under the 1200 ppm CO_2 concentration (a) Output voltage and (b) output current up to 5 cycles upon light-on process. (c) Output voltage and (d) output current up to 5 cycles upon light-off process.

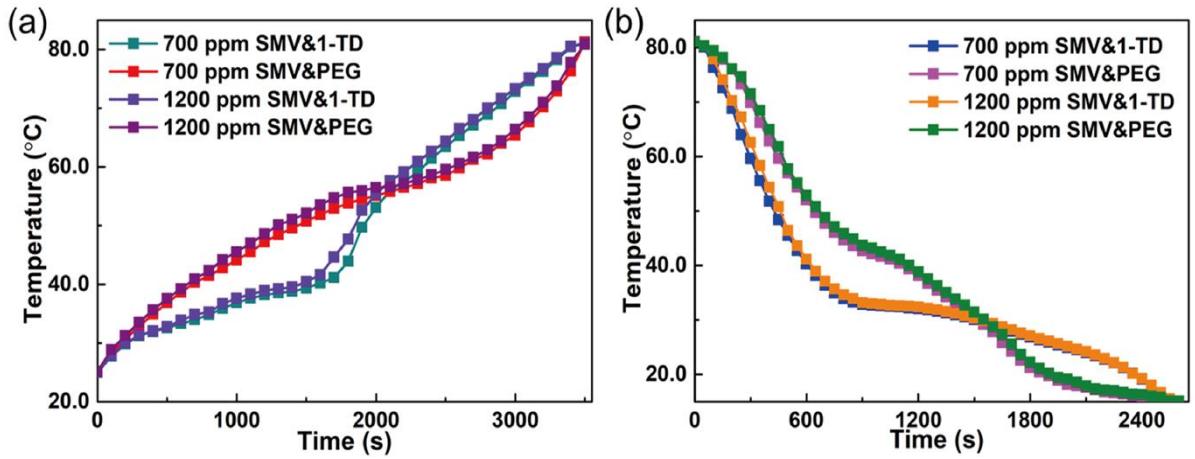

Fig. S43. The assembly made of RH 70% SMV supported 1-TD and RH 90% SMV supported PEG, the temperature profiles of 700 ppm and 1200 ppm two different CO_2 concentrations during (a) light-on process and (b) light-off process.

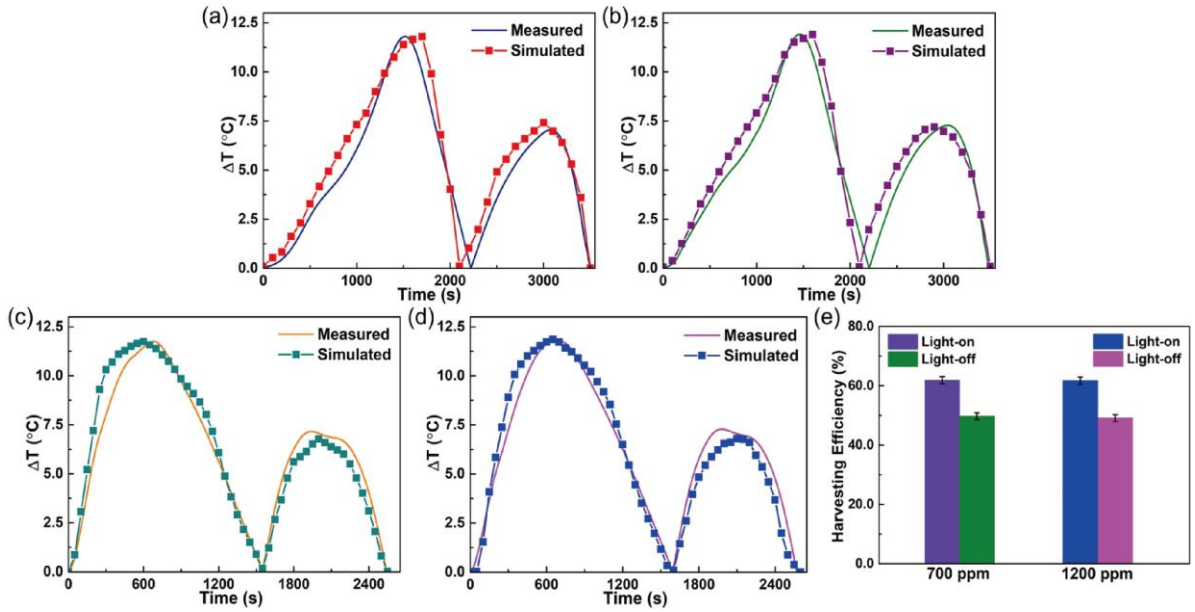

Fig. S44. The comparison of simulated result, temperature peaks during the light-on process with (a) 700 ppm CO_2 concentration and (b) 1200 ppm CO_2 concentration. For light-off process, (c) 700 ppm CO_2 concentration and (d) 1200 ppm CO_2 concentration. (e) The energy harvesting efficiency results at 700 ppm and 1200 ppm CO_2 concentration during light-on/-off process.